Bulletin of the Mineral Research and Exploration

http://bulletin.mta.gov.tr

Origin of the mineralizing fluids involved in the formation of the scheelite skarn in the Beleleita area (Edough NE, Algeria): Fluid inclusion and stable S, O and C isotope study

Abdelmalek LEKOUI[a*], Rabah LAOUAR[b], Djamel-Eddine AISSA[c] and Adrian Joseph BOYCE[d]

[a] *Laboratory of Geological Engineering (LGG), Faculty of Natural and Life Sciences, University of Jijel, 18000, Jijel, Algeria*
[b]*Département de Géologie, Faculté des Sciences de la Terre, Université Badji-Mokhtar Annaba, B.P. 12, 23000 Annaba, Algeria*
[c]*University of science et technology Houari Boumediene, Faculty of Earth Sciences, Geography and Territorial Planning, Algiers, Algeria*
[d]*Isotope Geosciences Unit, SUERC, East Kilbride, Glasgow, G75 0QF, Scotland.United Kingdom*

Research Article

Keywords:
Skarn, Stable Isotopes, Magmatic Fluids, Edough, Algeria.

ABSTRACT

This study investigates the first stable S-, O- and C-isotopes data on the Beleleita scheelite skarn deposit to assess the origin of the mineralising fluids involved in the formation of the skarn and related W-As-Bi-(Au) mineralisation. Two skarn bodies are embedded within the Neoproterozoic gneisses, south of the Edough metamorphic complex, NE Algeria. They show subparallel, discontinuous slabs (F1 and F2) approximately 700 m long and 10 m wide, striking NE–SW. The slabs were cross-cut by bore-hole drilling at a depth of 130 m during ORGM (Office de Recherche Géologique et Minière) mining exploration in the 1980s. Textural observations reveal two main cycles. Cycle I displays early classical zoned skarn assemblage, including clinopyroxene, garnet, plagioclase, pyrite, pyrrhotite, and chalcopyrite. Cycle II shows late lithiniferous and fluorinated skarn assemblage that corresponds to greisenised secant skarns, with fluorite, scheelite, lollingite, allanite, zinnwaldite series, sphene, wolframite, arsenopyrite, native bismuth, and quartz. Stable O-isotope analyses were carried out on both whole-rock samples and clinopyroxene, quartz, and garnet mineral separates, whereas C- and O-isotope analyses were conducted on gangue calcite. S-isotopes were carried out on sulphides (pyrite, chalcopyrite, lollingite and pyrrhotite). All the results display relatively narrow ranges ($\delta^{18}O_{SMOW}$ varying from +8.4 to +9.9‰; $\delta^{13}C_{PDB}$ ranging between -6.9 to -4.2‰ and $\delta^{34}S_{CDT}$ between -0.3 to +5.3‰), indicating a homogeneous source of fluids with significant magmatic signatures that contribute to skarn formation and ore deposition. Accordingly, the involved mineralising fluids most likely originated from the I-type magmatic event that prevailed during Burdigalian times in the Edough massif, similar to many other ore deposits in the area. Moreover, previous fluid inclusion studies carried out on fluorite, scheelite, and quartz of Cycle II show that the ores were deposited from hot (T_h = 500°-520°C), highly saline magmatic fluids under low pressure (0.5–0.6 kb), and this complies well with the present stable isotope data.

Received Date: 21.11.2023
Accepted Date: 04.09.2024

1. Introduction

The Edough metamorphic complex is a part of the internal zone of the North African Alpine belt, also known as “the Maghrebide” belt, whose current position is believed to be a consequence of Oligo-Miocene subduction and collision in the western Mediterranean between the African and European plates (e.g., Auzende et al., 1975; Cohen, 1980; Bouillin, 1986; Carminati et al., 1998, 2012; Caby et al., 2014). The core complex is locally overlain by

Citation Info: Lekoui, A., Laouar, R., Aissa, D. E., Boyce, A. J., 2024. Origin of the mineralizing fluids involved in the formation of the scheelite skarn in the Beleleita area (Edough NE, Algeria): Fluid inclusion and stable S, O and C isotope study. Bulletin of the Mineral Research and Exploration 175, 41-63. https://doi.org/10.19111/bulletinofmre.1543523

**Corresponding author: Abdelmalek LEKOUI, lekouim121@gmail.com*

sedimentary nappes, a structure resulting from the Oligo-Miocene subduction and collision processes.

The metamorphic complex of the Edough massif, structured in a NE-striking antiform (Figure 1b), is composed of a variety of Neoproterozoic and Paleozoic metamorphic rocks. The gneisses, which form the core, are thought to be originally calc-alkaline rocks (Ahmed-Said et al., 1993). The metapelites overlying the gneisses consist of two units: garnet- or more commonly kyanite-micaschist that alternate with metric slabs and layers of marble and skarns; and a Paleozoic upper unit (Ilavsky and Snopkova, 1987) comprising andalusite-bearing aluminous schists alternating with feldspathic quartzites. These lithologies have undergone a polycyclic metamorphism, from high pressure–high temperature (Cycle I) to low pressure–high temperature (Cycle III) conditions through medium pressure–medium temperature conditions (Cycle II) (Hammor, 1992; Bruguier et al., 2017). Undifferentiated mafic and ultramafic rock outcrops in the La Voile Noire and Bou Maiza localities are tectonically incorporated within gneiss (Hadj-Zobir and Oberhansli, 2013; Bosch et al., 2014). The nappes consist of Cretaceous sandstones, shales, and marls as well as Oligo-Miocene sandstone flysch.

The Edough core complex and the overlying sedimentary rocks were intruded by igneous lithologies around 16 Ma (Marignac and Zimmermann, 1983). These igneous rocks are divided into two groups: rhyolitic domes and veins and subvolcanic microgranitic intrusions. Their geology, geochemistry, and petrogenesis were studied by Ahmed-Said et al. (1993) and Laouar et al. (2002), who determined that they are metaluminous I-type lithologies are indicative of mantle-derived magmas with a small amount of crustal material.

The magmatic and associated hydrothermal events in the Edough massif are thought to have resulted in four types of mineralisation: (1) base metal vein mineralisation, such as the largest Ain Barbar ore deposit in the area, which is not currently operated, and El-Mellaha (e.g., Bolfa, 1948); (2) skarn W-As-Au-related mineralisation, such as that of Beleleita (Aissa et al., 1995); (3) Fe-Pb-Zn-Cu deposits related to the skarns and amphibolites of Boumaiza and Berrahal region; and (4) Sb-Au veins occurring within the metamorphic complex (e.g., Koudiat El Ahrach; Saf-Saf and Ain Barbar). Some of the Edough ore deposits were extensively worked in the past, and veins in the core complex were recently prospected for Au-W-As.

The Beleleita (Karézas) scheelite-skarn deposit is located in the southern part of the Edough massif. The deposit is composed mainly of rare metal concentrations, such as W, Sn, Bi, Li, and F, in addition to As and Au, which are related to arsenopyrite [SO. NA.RE.M (Société Nationale de Recherche Minière), 1975]. The skarn bodies have been investigated in terms of their mineralogy, geochemistry, and geochronology, as well as fluid inclusions (Bouguerra, 1990; Aissa, 1996; Aissa et al., 1999; Marignac et al., 2016). The contact between the skarns and the magmatic body is not observed at the surface, however fluid inclusion data and K-Ar dating results show that the skarns were formed at circa 17 Ma by high-temperature, high-salinity, and low-pressure magmatic fluids (Aissa et al., 1995; Marignac et al., 2016). Moreover, Laouar et al. (2002) indicated that the fluids responsible for the marble skarnification were most likely derived from a buried I-type granitoid related to the Late Burdigalian igneous event in the Edough massif. Such a magmatic fluid is also responsible for the most common occurrences of scheelite skarns. To shed more light on the genesis of the Beleleita skarn deposit, Aissa (1997) and Laouar (2002) recommended further studies using stable S-, C- and O-isotope geochemistry, along with previous findings on fluid inclusions.

In this paper, we present for the first time the O-, C-, and S-isotope data obtained from whole-rock mineral separates and sulfide minerals of the Beleleita skarn lithologies. The petrology, metallography, and previous fluid inclusions are constrained to the isotopic data to elucidate the characteristics and origin of the fluids responsible for both skarnification processes and ore deposition. The isotopic data are then compared to those of the Edough metamorphic and magmatic rocks to evaluate the role of the Miocene magmatic and metamorphic events in the generation of these fluids.

2. Geology

The Beleleita massif, located about 12 km southwest of Annaba city, corresponds to the southernmost metamorphic block of the Edough complex (Figure 1a). As a part (10 x 4 km) of the Edough metamorphic complex, the Beleleita massif (Figure 1b) is formed by several types of regionally metamorphosed and locally metasomatised rocks, with varying degrees of metamorphism. The outcropping metamorphic lithologies, which derive from the Neoproterozoic to the Paleozoic Ages, are dominated by migmatised augen gneisses with levels of leptynites and quartzites; two mica gneisses; andalusite-, kyanite-, staurolite-, and garnet-bearing micaschists containing slabs of marbles, amphibolites, and skarns.

The augen gneisses are well-foliated rocks and often experience severe kaolinisation near the faults and fracture zones. The two mica-gneisses show meter-thick layers with a N50°–N80°-directed foliation. In addition to their classical mineralogy of quartz, K-feldspar, micas (muscovite and biotite), plagioclase, and occasionally garnet, they may contain prismatic (2 to 5 mm) tourmaline minerals. The common and most striking chemical feature of the Beleleita gneisses is that they contain anomalous concentrations of Sn, W, B, Rb, Li, and F compared to other gneisses of the Edough metamorphic massif (Aissa, 1996).

The micaschists outcrop in the southeastern part of the Beleleita massif unconformably overlap the augen gneisses. They are composed mainly of muscovite, biotite, feldspar, and quartz, in addition to metamorphic minerals such as andalusite, staurolite, and garnet. Lenses of marble, skarns, and amphibolites are also observed within these micaschists. Marbles crop out as metric lenses within the gneisses and micaschists. They are mainly composed of calcite (88%), with accessory phlogopite, magnetite, graphite, and pyrite.

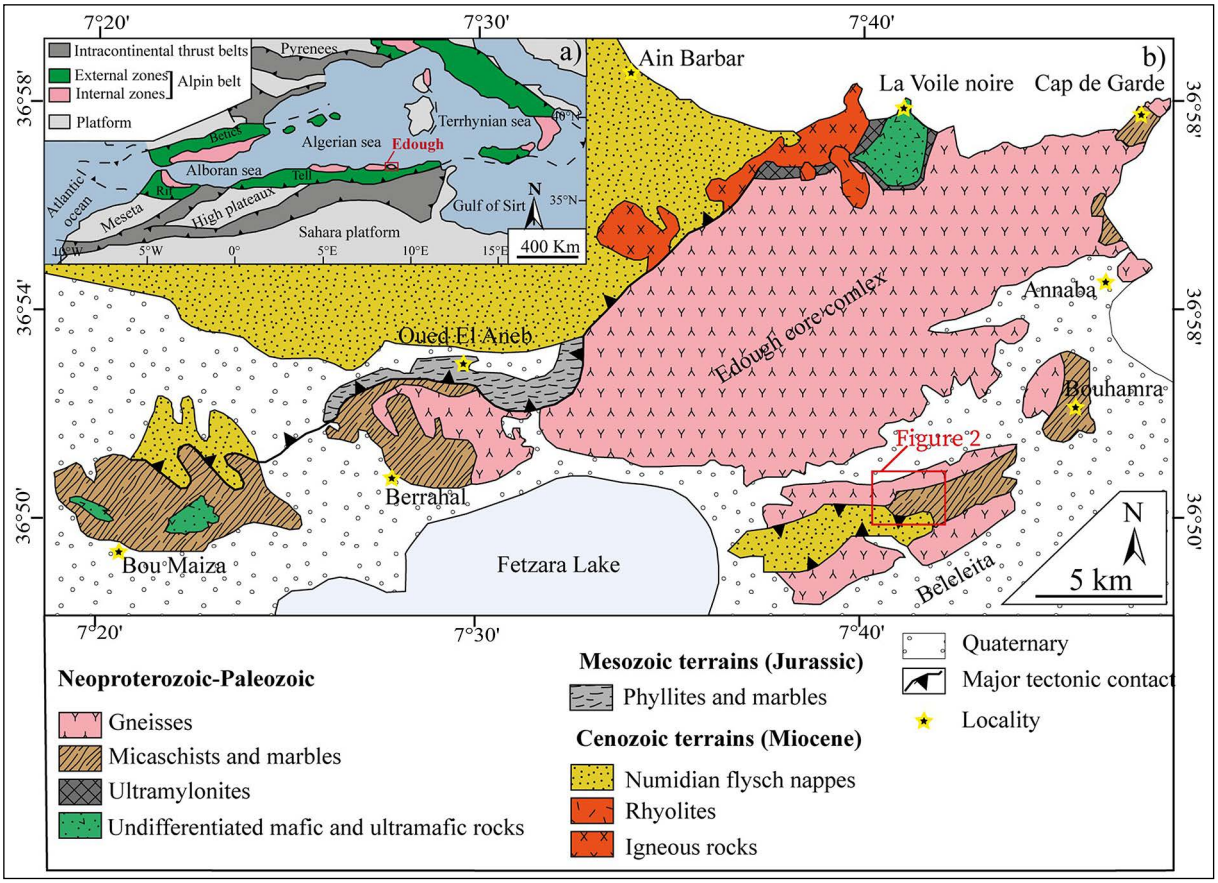

Figure 1- a) Location of the Edough complex within the Alpine belt (Durand-Delga, 1980), b) Simplified geological sketch map of the Edough complex showing the study area in the Beleleita massif.

Pegmatites and aplites develop widely in the Beleleita region; they intrude gneisses along fault zones and tectonic contacts. They are tourmaline- and muscovite-bearing rocks often outcropping along the NNE–SSW–oriented faults. Skarns develop mainly on marble protoliths and include pyroxenites, garnetite, and—to a lesser extent—amphibolites. Contact with the gneisses is often marked by the formation of plagioclase-bearing skarns or plagioclasites. The exposed sedimentary rocks consist solely of the Miocene sandstones from the Numidian nappes, which outcrop at the southern part of the massif and overlay unconformably the metamorphic formations.

The metamorphic lithologies of the Beleleita massif were subject to intense faulting and fracturing that facilitate hydrothermal fluid circulation, as well as the emplacement of highly differentiated igneous rocks, such as the observed swarms and lenses of pegmatites and aplite bodies. As a whole, the structural framework of the Beleleita ore deposit is defined by two major, large-scale fault systems: (1) parallel faults trending from E–W to NNE–SSW along with schistosity fabrics, dipping at 55°–70°, which postdate the skarn bodies and pegmatite lenses; and (2) faults trending from N–S to roughly NW–SE, which crosscut the first fault system and show subvertical dipping (75°–90°). Some minor faults could also be observed in the area.

2.1. Ore Deposit Geology

The Beleleita W-As skarn deposit has been mined since 1930, when the deposit provided only arsenic (lollingite). Wolfram (WO_3 at 0.97%) was discovered in the 1950s. However, the enrichment process allowed the extraction of small amounts of W minerals (less than 30%), which led to the mine closing later. Recently, several research and exploration surveys have been carried out in this area (e.g., E.RE.M. (Entreprise de Recherche Minière), 1969; Aissa, 1996; Aissa et al., 1998).

Geologically, the Beleleita W-As skarn ore deposit is composed of two ~10 m thick and slightly parallel skarn formations (F1 and F2; Figure 2); they are 600–700 m long and more than 130 m deep. These formations are hosted by metamorphic gneisses of the Beleleita region that are composed mainly of monotonous paragneisses and, less commonly, leucocratic orthogneisses. The petrographic study of 30 representative bore-hole skarn samples reveals four lithological facies.

1. Pyroxenites: These are the most abundant skarn lithologies. They develop at the outer parts of the marble host rock and show irregular and sharp contact with the marble foliation. The pyroxenites display mostly massive (Figure 3a) but rarely banded textures (Figure 3b), especially near the contact with the gneisses. However, the contact marble-skarn is marked by a garnet zone (xenomorphic or subhedral rounded crystals), followed by aggregates of clinopyroxenes of hedenbergitic composition. Clinopyroxene is the dominant calc-silicate mineral that develops widely in the skarn zones, and it often shows acicular or prismatic aggregates (~5 mm), though rare euhedral to subhedral crystals (Figures 4a, b) may also be observed. Massive pyroxenites often contain sulphide minerals, such as pyrrhotite, chalcopyrite, and pyrite. Phlogopite fine relics within clinopyroxene aggregates may indicate the composition of the marble protolith (Figure 4c). Centimetre- to millimetre-thick space-filling fluorite-lollingite-scheelite-sphene veins often cross-cut the pyroxenite rock (Figure 4a). Clinopyroxenes are replaced in places by hydrous minerals, such as zoisite and amphibole, which develop along clinopyroxene crystal edges (Figure 4h).

2. Garnetites: They are less abundant compared to pyroxenites and occur as massive (Figure 3a) rocks composing mainly of xenomorphic to polygonal garnet crystals (Figures 4e, f). The latter are often fractured and zoned and have a grossular-almandine composition in the core and a grossular-andradite at the rim (Aissa, 1996; Aissa et al., 1998, 1999). Garnetites may also occur as centimetre-thick bands, where the rounded and twinned but often zoned garnet crystals are associated with interstitial calcite minerals (Figures 4e, f). The occurrence of interstitial and calcite veins replacing garnet minerals indicates that the skarn underwent protracted interaction with the fluids (Li et al., 2019). In addition to garnet, euhedral clinopyroxene, amphibole, and minor K-feldspar may occur within the garnetites. Epidote develops at the expense of retrograde hydrous garnet alteration along microcracks, simultaneously with the deposition

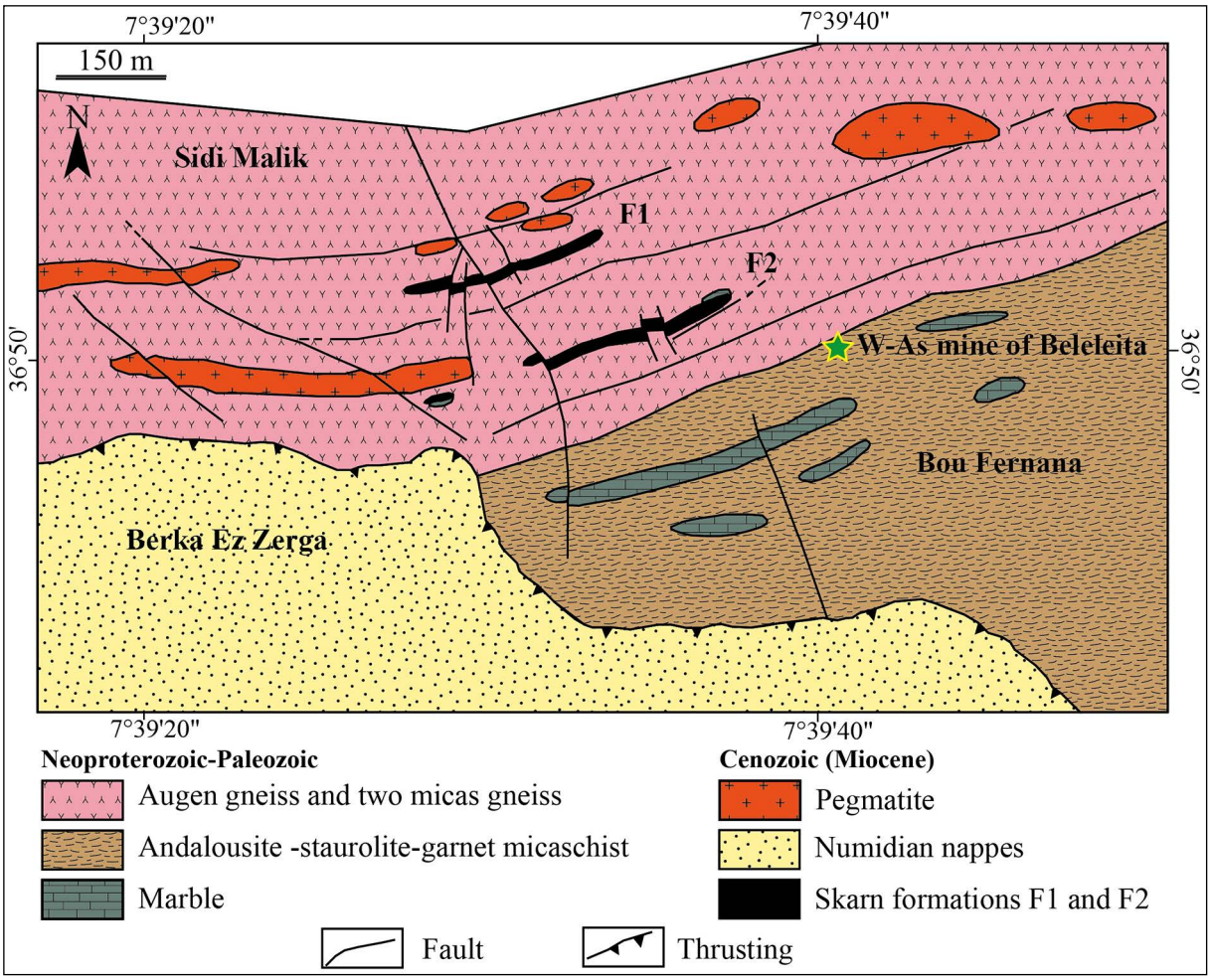

Figure 2- Simplified geological map of the Beleleita area showing the occurrence of the skarn formations F1 and F2 (E.RE.M., 1969; Aissa, 1996; Aissa et al., 1999; Marignac et al., 2016)

of interstitial fluorite and sulphide minerals. These garnetites are highly enriched in Sn and rare metals (Aissa, 1996; Aissa et al., 1998), which is common in most W-skarn deposits (e.g., Einaudi and Burt, 1982; Xue et al., 2021).

3. Amphibolites: These often feature massive texture and a relatively light-green colour (Figure 3d). Amphibolites possess nemato-granoblastic texture, where amphibole aggregates take the form of large xenomorphic grains to subhedral crystals (Figures 4g, h). Amphiboles are composed of ferro-pargasite and edenite (Aissa, 1996; Aissa et al., 1998, 1999). In places, the amphibole (hornblende) replaces clinopyroxene (uralitisation), where relics of clinopyroxene are observed within the hornblende minerals (Figure 4g). Epidote is often the alteration product of amphiboles within the amphibolite zone.

4. Plagioclasites: They occur as thin layers, often alternating with bands of greenish pyroxenites (Figure 3b), and usually develop at contact with the gneisses. Hand-specimens display a fine-grained rock of whitish colour, composed mainly of intermediate to calcic plagioclases. The plagioclase generally shows prismatic subhedral twinned and zoned crystals (Figure 4d). It can also occur as xenomorphic grains, frequently crosscut by fluorite veins, and may be replaced by K-feldspar through K input from the inflowing fluids (Figure 4j).

2.2. Ore Mineralogy

The W-As mineralisation related to the Beleleita skarns is believed to be controlled by two main geological features: (1) a structural character related to faulting and fracturing used as a pathway for

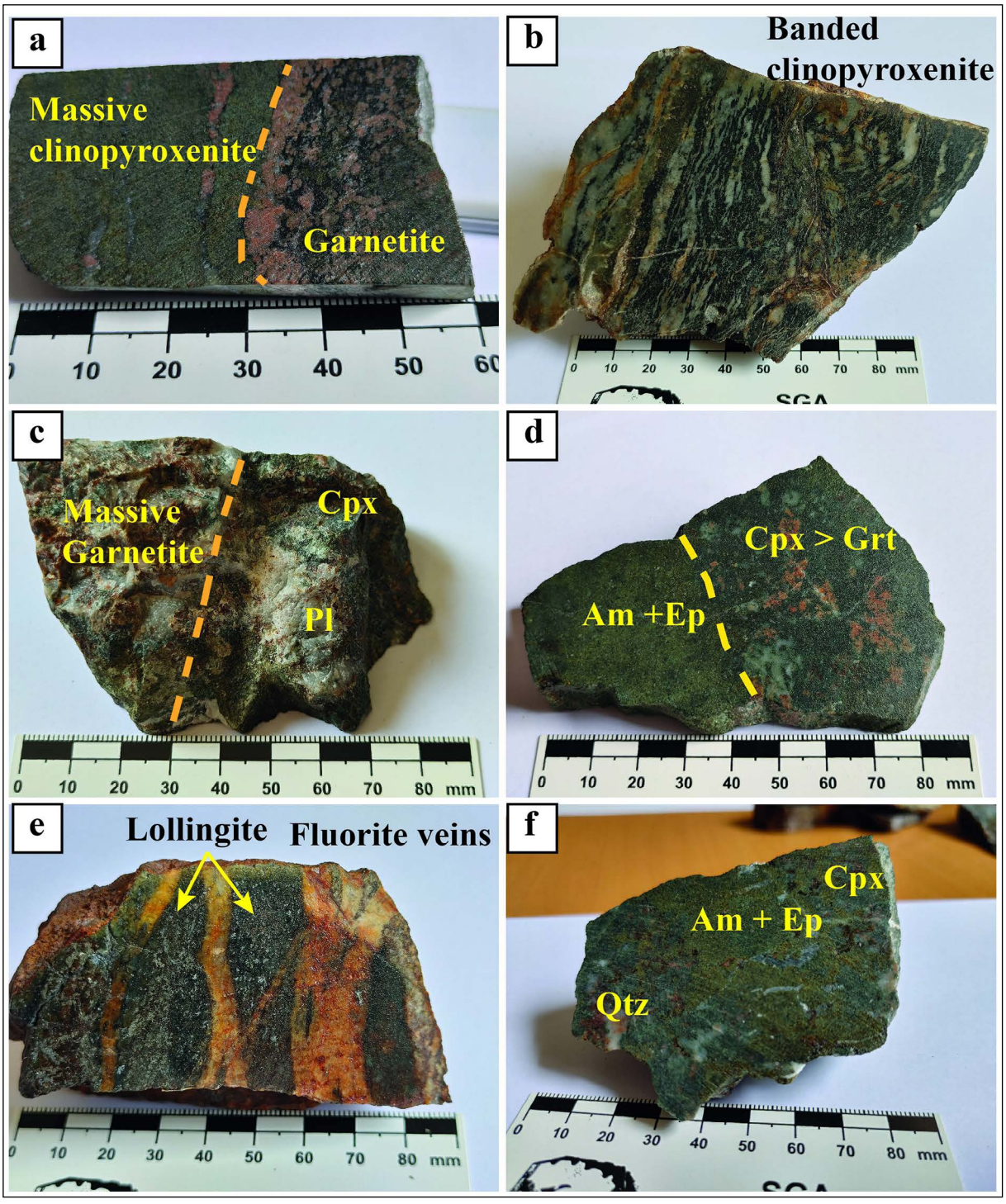

Figure 3- Selected macrophotographs of the Beleleita skarn showing the skarn lithologies; a) massive, zoned skarn with clinoproxenites and garnetites, b) banded clinopyroxenites overprinted by plagioclasites, c) massive garnetite with clinopyroxene (Cpx) and plagioclases (Pl), d) clinopyroxene (Cpx)-garnet (Grt) skarn zone in contact with amphibolite (Am= and epidote (Ep), e) fluorite veins and crosscutting clinopyroxenite with lollingite development, f) development of interstitial quartz (Qtz), amphibole (Am) and epidote (Ep) along microcracks of clinopyroxenite (Cpx).

hydrothermal fluid circulation, and (2) a lithological character related to the porous nature of the marbles as well as their high reactivity with hydrothermal solutions. They are therefore considered a favourable environment for ore deposition.

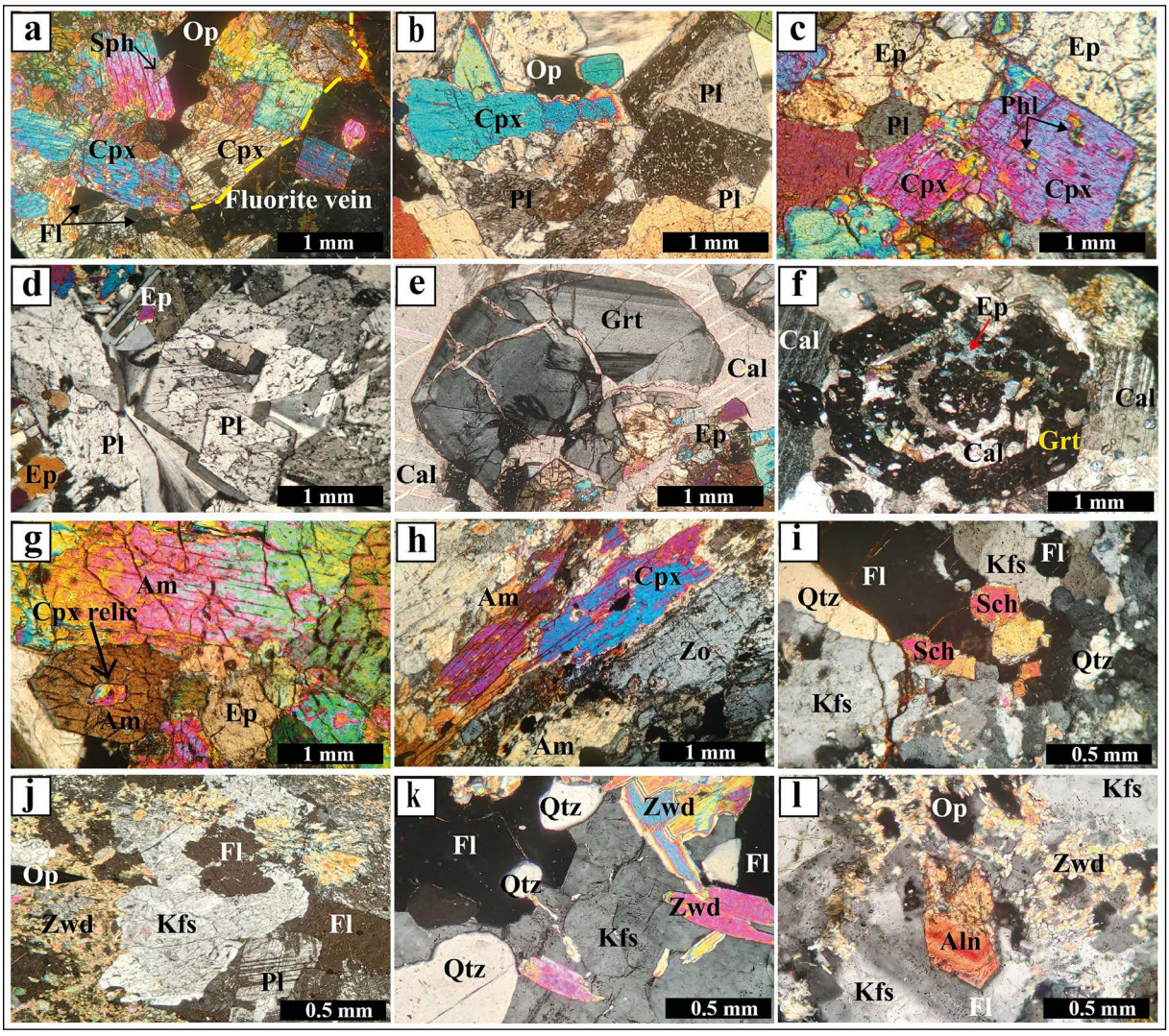

Figure 4- Selected microphotographs of the common skarn textural patterns of the Beleleita area under transmitted light microscope; a) massive clinopyroxenite with euhedral prismatic clinopyroxene (Cpx) crosscut by fluorite (Fl) vein and xenomorphic interstitial fluorite, b) zoned plagioclase (Pl) associated to prismatic clinopyroxene, c) Epidotized clinopyroxene with thin inclusions of phlogopite (phl), d) Plagioclasite with zoned crysts (Pl) and epidote (Ep), e) Twined garnet in rounded crystals replaced by epidote (Ep) and calcite (Cal) along microcracks, f) Zoned crystal of garnet (Grt) replaced by epidote and calcite, g) microscopic aspect of the amphibolite with euhedral crysts of amphibole (Amp) hosting relic of clinopyroxene (uralitisation), h), clinopyroxene crystal replaced by amphibole (Amp) and zoisite (Zo), i) fluorite (Fl) vein associated with scheelite aggregates (Sch), K-feldspar (Kfs) and quartz (Qtz), j) plagioclase (Pl) invaded by fluorite (Fl) and replaced by K-feldspar (Kfs) and zinwaldite (Zwd), k) massive deposition of K-feldspar (Pl) and zinwaldite (Zwd) along with fluorite (Fl), quartz (Qtz) and opaques (Op), l) euhedral crystal of allanite associated with fine zinwaldite, opaques (Op) and large patches of k-feldspar (Kfs).

Investigations carried out on polished sections under a reflected light microscope of selected mineralised skarn samples indicate a number of replacement processes. The following observations are particularly notable.

Lollingite is the most abundant sulphide mineral in the Beleleita skarn. It mostly occurs as fractured millimetre-size grains (up to 10 mm) that show a massive texture (Figure 5a). Large, isolated subhedral crystals are also observed as inclusions within the clinopyroxene crystals of the pyroxenites (Figure 5c).

Pyrrhotite is the most widespread sulphide in the Beleleita skarns; it shows millimetre- to centimetre-sized grains disseminated throughout the rock (pyrrhotite I; Figure 5d). Pyrrhotite may also occur as millimetre-thick veins (pyrrhotite II; Figure 5e).

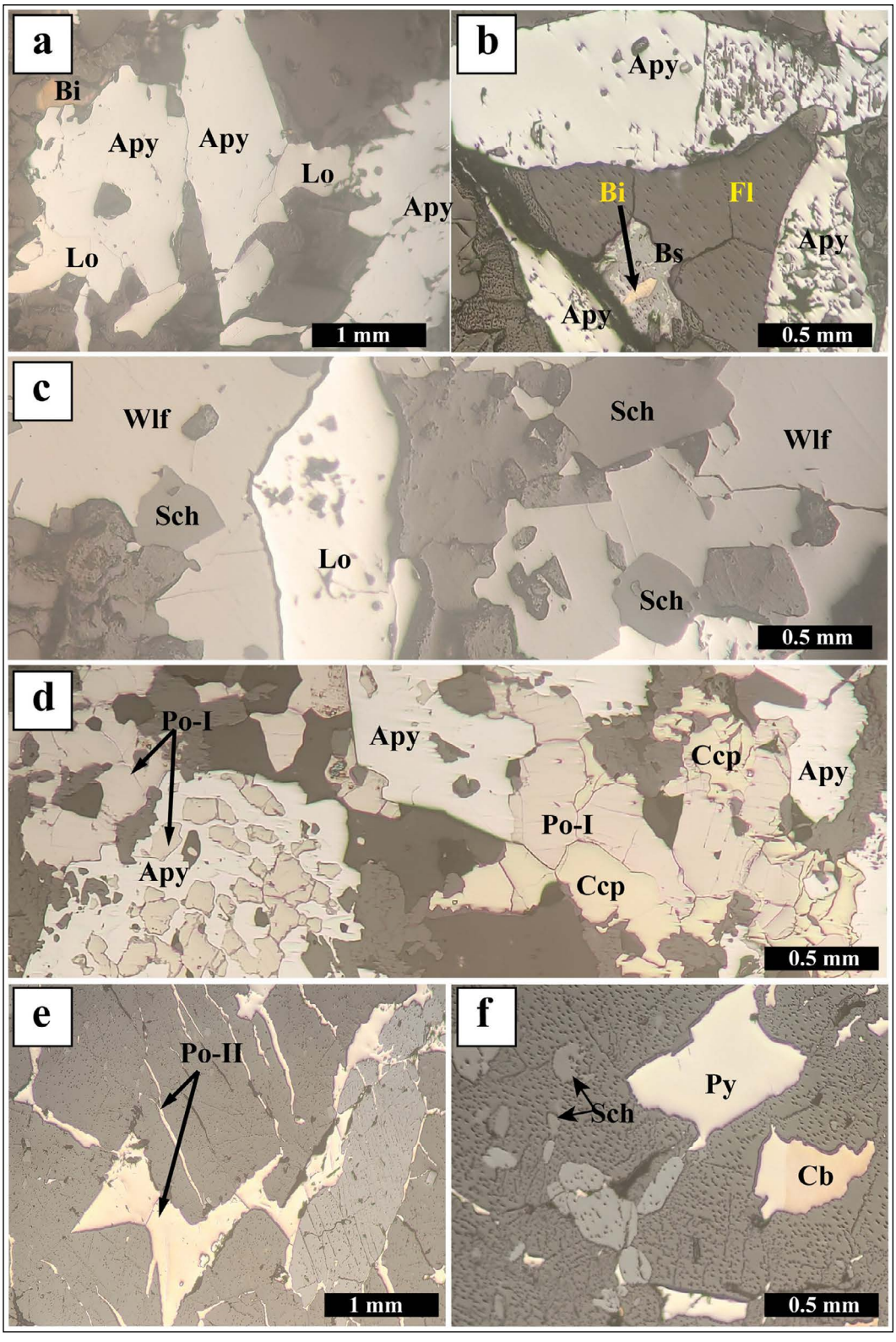

Figure 5- Selected microphotographs showing the principal textural patterns of the scheelite skarn ore of Beleleita; a) replacement of lollingite (Lo) (yellowish color) by arsenopyrite (Apy) (white color), b) replacement of bismuth creamy (Bi) by bismuthinite medium grey (Bs) associated to isolated euhedral crystals of arsenopyrite (Apy), c) large patches of wolframite (Wlf) (brownish grey) replacing scheelite (sch) (dark grey), d) massive pyrrhotie I (Po) replaced by arsenopyrite (Apy) and chalcopyrite (Ccp), e) interstitial and millmetric veins of pyrrhotite II (Po), f) disseminated grains of pyrite (Py), cubanite (Cb) creamy and scheelite (Sch).

Pyrrhotite I is coeval with the retrograde stage of Cycle I, whereas pyrrhotite II occurs during the beginning of the prograde stage of Cycle II.

Scheelite exhibits isolated xenomorphic grains that are often disseminated in the rock (Figure 5c). It also occurs as millimetre-sized aggregates. Arsenopyrite develops at the expense of both pyrrhotite and lollingite, where it is replaced and corroded at the edges of the crystals (Figures 5a, d). Wolframite is a rare secondary mineral that often replaces scheelite aggregates. It occurs as large millimetre-sized crystals (Figure 5c). Chalcopyrite develops at the expense of pyrrhotite I and pyrrhotite II; the replacement process often occurs at the outer parts of the pyrrhotite grains (Figure 5d). Pyrite is a rare mineral compared to other sulphides; it shows subhedral grains disseminated within the rock or occurs as a space-filling mineral (Figure 5f).

Native bismuth and bismuthinite are commonly associated with each other; the latter may partially or totally transform into native bismuth (Figure 5b). Fluorite occurs as veins of various thicknesses (up to 2 cm). Fluorite crystal softens primary minerals such as garnets, pyroxenes, and plagioclases. Fluorite may also occur as interstitial grains within the pyroxenite minerals (Figure 5b). Cubanite is commonly associated with pyrite and pyrrhotite; it is rare and shows fine-grained aggregates (less than 0.5 mm).

2.3. Skarn and Ore Formation

Petrographic observations and mineral textures reveal two cycles of hydrothermal activity (Cycle I, II) which directly involved in skarn formation and associated W-As mineralisation. Each cycle shows two prograde-retrograde skarn stages.

The prograde skarn stage of Cycle I is characterised by the formation of zoned skarns at the contact between the marbles and the host gneisses. The marble mineralogy is replaced by clinopyroxenes (ferrosalite-hedenbergite; Aissa, 1997) that form pyroxenites facies and grossular-andradite garnet, which forms the garnetites, with high pyroxene/granet ratios. The two-mica-gneiss parageneses are replaced by An_{60}-plagioclase that comprise the plagioclasites. The retrograde skarn stage is marked by the development of calcic amphibole and zoisite at the expense of clinopyroxene, epidote, and calcite at the expense of garnet, and the deposition of sulphide minerals such as pyrite, pyrrhotite, chalcopyrite, and cubanite.

Cycle II mineral paragnenesis is mainly observed within the fracture zones at the contact point between the plagioclasites of Cycle I and the two-mica-gneisses. The prograde stage paragenesis of this cycle comprises fluorite and Mo-free scheelite, which develop at the expense of plagioclase and result in K-feldspar formation. The prograde stage begins with the appearance of sulphur-rich lollingite ($Fe_{0.99}As_{1.88}S_{0.12}$; Aissa, 1996), allanite, and Li-F-rich micas (the zinnwaldite series) followed by the replacement of scheelite by wolframite and lollingite by As-rich arsenopyrite (35.5% As). Native bismuth and bismuthinite also belong to this stage. The retrograde stage is marked by severe silicification process that is observed either as quartz veins or as massive quartz replacements of plagioclase.

Cycle II features, such as the Li-F-enrichment of newly formed minerals, are comparable to those typical of 'greisenised skarns' (Kwak, 1987) and display similar characteristics to the intermediate 'W-F skarns' defined by Newberry (1998). An equilibrium temperature for the lollingite-arsenopyrite has been estimated at 450°C ± 30°C using the method of Kretschmar and Scott (1976). $^{39}Ar/^{40}Ar$ dating on Cycle II Li-rich micas gave an age of 16.9 ± 0.4 Ma, corresponding to the Late Burdigalian period, which falls within the range of the post-collisional magmatic event in northeastern Algeria (from 17.02 ± 0.06 to 12.91 ± 0.31 Ma; Abbassene et al., 2016, 2019); indicating that Beleleita W-As mineralisation occurred just after the end of the extensional tectonic events. The petrographical and metallographical results enable the establishment of a paragenetic sequence of the skarns and associated W-As mineralisation, as shown in Figure 6.

3. Materials and Methods

Data for the fluid inclusion study were taken from Aissa (1996), Aissa et al. (1998) and Marignac et al. (2016). Microthermometric measurements were carried out on primary fluid inclusions (10 and 100 μm size) in fluorite and scheelite from the prograde

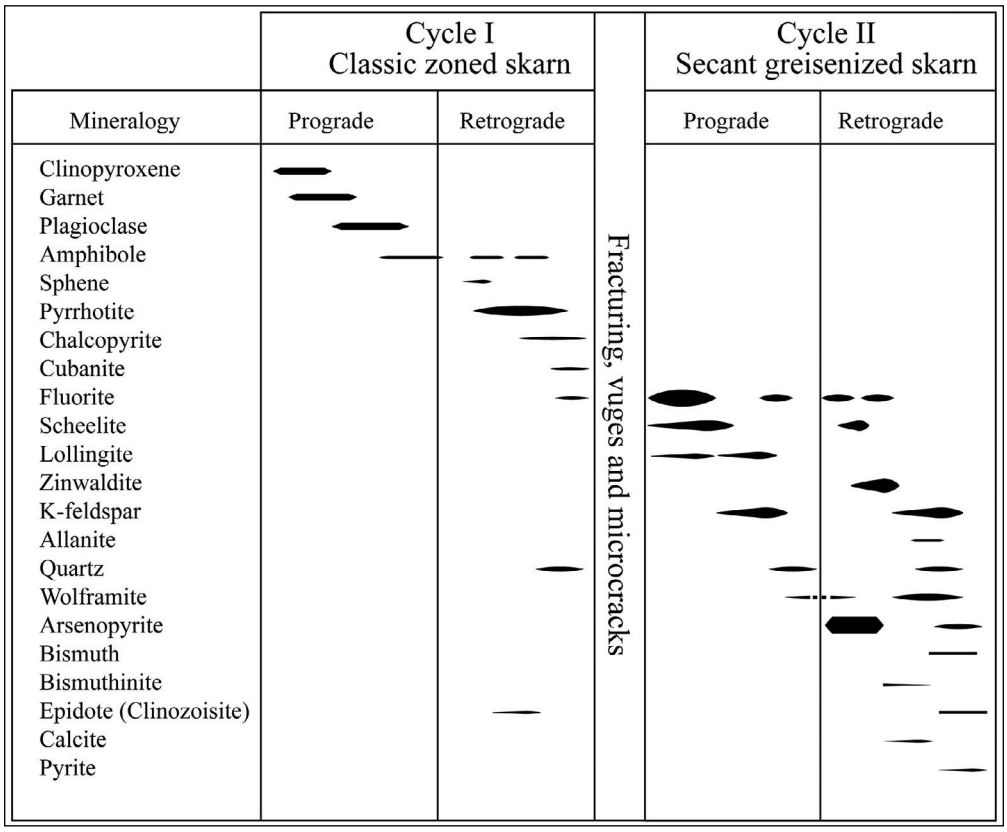

Figure 6- Paragenesis of mineral assemblages showing the evolution of skarn and mineralization of Beleleita.

stage and on quartz from the retrograde stage: Both from Cycle II, the main mineralising cycle.

Stable isotope analyses were carried out at the Scottish Universities Environmental Research Centre (SUERC), East Kilbride, Glasgow. Twelve sulphide separates were prepared for S-isotope analyses: Five samples from the Beleleita mineralised skarns and seven samples from different lithologies and localities of the Edough metamorphic complex (six sulphides from several marble outcrops and one from the Cap de Garde reaction skarns). Thirteen samples were selected and prepared for O-isotope analyses: 11 silicate mineral separates (pyroxene, garnet, and quartz) from both Cycle I and Cycle II assemblages of the skarn, one whole-rock sample from the skarn, and one quartzite sample from the Edough basement. Two calcite minerals (one from the skarn and one from the host marbles) were selected for both the O- and C-isotopic compositions.

For sulphur isotope analyses, the sulphide samples were combusted with excess Cu_2O at 1075°C to liberate the SO_2 gas under vacuum conditions. Liberated SO_2 gases wereanalysed on a VG Isotech SIRA II mass spectrometer, with standard corrections applied to raw $\#^{66}SO_2$ values to produce true $\#^{34}S$. The international NBS-123, IAEA-S-3, and SUERC standard CP-1 standards were employed. The reproducibility of the results based on complete repeat analyses was ± 0.3 ‰ (1σ).

For oxygen isotope analyses on silicate and whole-rock samples, laser fluorination with excess ClF3 was used. The released O_2 was converted to CO_2 through a reaction with hot graphite, as described by Clayton and Mayeda (1963) and Borthwick and Harmon (1982), and then analysed online using a VG PRISM III spectrometer. Reproducibility was better than ± 0.3‰ (1σ) based on repeated analyses of internal laboratory standard SES 1 ($\delta^{18}O$ = +9.6‰).

C- and O-isotope analyses of calcite samples were carried out on an automated continuous flow VG Prism Series II Isotope Ratio Mass Spectrometer using international standard IAEA-CO-8 (calcite) and

internal standard MAB2C. Reported analyses are each the mean of four values.

The stable isotope data, along with the sample location, are given in Tables 2, 3, and 4. S-isotope results are reported in the 'delta' (δ) notation as per mil (‰) deviations relative to Vienna Canon Diablo Troilite (V-CDT), the O-isotope data are reported as per mil (‰) deviations relative to Vienna Standard Mean Ocean Water (V-SMOW), and carbon isotope ratios were calibrated to Vienna Pee Dee Belemnite (V-PDB).

4. Results

4.1. Fluid Inclusions

Based on the observed fluid phases at room temperature (~ 25°C), three types of fluid inclusions (FIs) were identified: Type I, Type II, and Type III (Table 1). These FI types occur in fluorite, scheelite, and quartz of Cycle II, coexisting in their host minerals. Type I FIs are two-phase liquid-rich (L) homogenising in the liquid state. Type II FIs are two-phase vapour-rich (V) homogenising in the vapor state, consisting mostly of carbonic vapour (CO_2). Type III FIs are multiphase inclusions consisting of liquid, vapor, and solid (daughter minerals; L+V+S) phases. Type III FIs are liquid and feature a volatile component through clathrate melting and daughter minerals homogenising in the liquid state. Daughter minerals commonly include halite and sylvite.

Bulk homogenisation temperatures (T_h) are comparable to almost all analysed mineral phases (Figure 7). Temperatures of FIs in quartz range between 300°C–540°C, those for scheelite vary between

Table 1- Microthermometric data from the fluorite, scheelite and quartz minerals of the Beleleita W-As skarn mineralization. L >V: Liquid-dominated fluid inclusion homogenizing in liquid state; VCO_2 > L: Vapor-dominated (mostly CO_2) fluid inclusion homogenising in vapor state; L > +V+S : Liquid-dominated fluid inclusion containing a solid phase homogenizing in liquid state; L> + VCO_2+S: Liquid-dominated fluid inclusion containing a solid phase homogenising in liquid state; V> + L+S: Vapor-dominated fluid inclusion containing a solid phase homogenising in vapor state.

Type		Tm-CO_2 (°C)	Te (°C)	Tm-ice (°C)	Tm-clathrate (°C)	Tm-halite (°C)	Th (°C)	Salinity (Wt% NaCl)
Quartz								
Type I	L >V	-	-68/-31	-19/-25	-		317/550	9.2 - 16.04
Type II	V_{CO2} > L	-57/-62	-25/-49	-6/-9	2/9		309/535	1.3 - 10.5
Type III	L > +V+S	-	-68/-57	-40/-18	-	158/311	302/543	28 - 35
	L> + V_{CO2}+S	-67.5	-39	-18	-4.2/-2.1		372/415	-
	V> + L+S	-69/-76	-42/-48	-	-		386/532	-
Fluorite								
Type II	V_{CO2} > L	-57/-59	-22	-1	9		372/502	0.42
Type III	L > +V+S	-	-53/-26	-42/-18	5.6		419/427	-
	L> + V_{CO2}+S	-60	-25	-18		404	423	-
	V> + L+S	-59/-58	-37/-24	-26/-8	-8/15	154/287	369/526	29.84 -4 6.42
Scheelite								
Type I	L >V	-	-21/-38	-16/-5	-		334/378	6.43 - 12.87
Type II	V_{CO2} > L	-65/-57	-44		5/9		310/397	-
Type III	L > +V+S	-	-25/-43	-7/-30	-	112/198	329/416	28.4 - 31.80
	L> + V_{CO2}+S	-	-43	-	-	279	371/376	36.48
	V> + L+S	-68/-57	-46/-34	-26/-16	1/3		402/423	-
Composition of the volatile phase in quartz								
	Type	ZCO_2	ZCH_4	ZN_2				
	Type II	57.1	24.8	18.1				
	Type III	49.9	36.5	21.6				
	Type III	50.0	50.0	0.0				

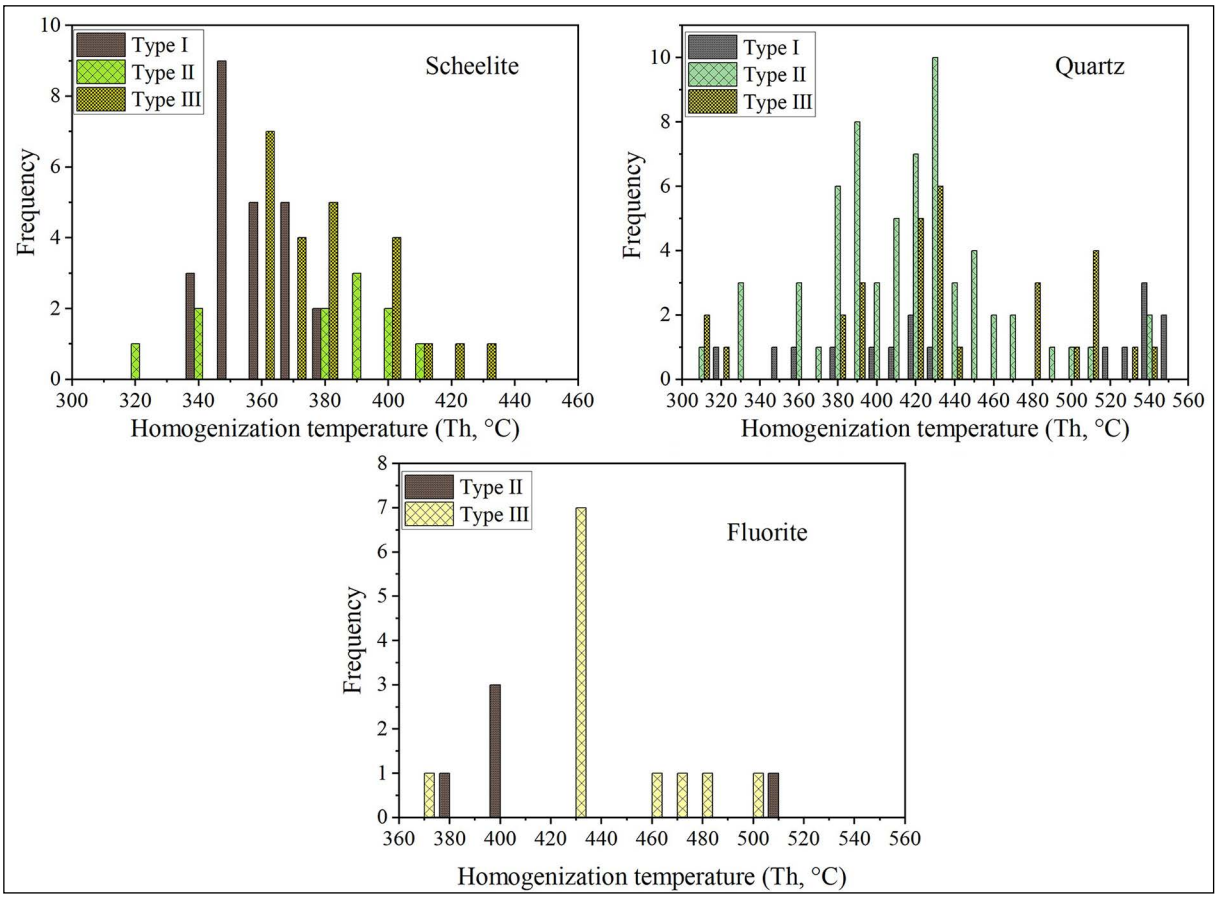

Figure 7- Histograms showing the distributions of homogenization temperatures of fluid inclusions in quartz, fluorite, and scheelite minerals of the Beleleita W-As skarn.

320°C–430°C, and those for fluorite are between 360°C–540°C. Salinity values are also comparable for the FIs of the three minerals. They range from 15 to 46 wt% NaCl. The highest salinities (up to 46 wt% NaCl) are recorded in both the daughter mineral-bearing FIs (Type III) and the volatile-bearing FIs of Type II. On the other hand, lower salinities (< 10 wt% NaCl) were observed in type I FIs (liquid-bearing FIs), which are hosted in quartz from the retrograde stage of Cycle II.

The first melting temperatures are often very low. The measured eutectic temperatures (T_e) range from -25°C to -48°C. During the freezing/heating processes, bulk CO_2 melting occurs at very low temperatures, ranging from -69.0°C to -57.0 °C (Table 1), indicating the presence of methane gas (CH_4; Soloviev and Kryazhev, 2018). Raman spectrometry carried out by Aissa (1996) revealed the presence of both CH_4 and N_2. Ca/Na ratios oscillate between 0.2 and 0.9. Using the dissolution temperatures of halite and sylvite, the K/Na ratios, which are determined on the H_2O-NaCl-KCl system according to Sterner et al. (1988) method, yield values higher than 1 (up to 1.7).

4.2. Stable isotopes

$\delta^{34}S$ values of the skarn sulphides are almost homogenous and present a narrow range of variation, between -0.34‰ and +1.8‰, with one lollingite sample from Cycle II paragenesis that displays a relatively high $\delta^{34}S$ value of +5.19‰. On the other hand, the sulphur isotopic composition of sulphides from metasedimentary rocks of the Edough complex, such as those of the marbles from Beleleita, Boumaiza, Bouhamra, and Cap de Garde, as well as a sulphide sample from the reaction skarns of Cap de Garde, is depleted in $\delta^{34}S$, exhibiting negative $\delta^{34}S$ values. These cover a wide range of variation, from -17.4‰ to -7.3‰ (Table 2).

Table 2- Sulphur isotopic composition of sulphides from the Beleleita scheelite skarn.

Sample No	Mineral	$\delta^{34}S_{V\text{-}CDT}$ (‰)	Comments
BEL1-GAL10	Pyrite	+1.7	Mineralized skarn (Beleleita)
BEL2-GAL10	Pyrite	+1.8	
04 SK IIc	Pyrite	+0.04	
04 SK IIb	Chalcopyrite	-0.34	
04 SK Ia	S-loellingite	+5.19	
04 CIP 01	Pyrrhotite	-14.85	Marble (Beleleita)
03 BHR 2	Chalcopyrite	-7.36	Marble (Bouhamra, Edough)
03 BHR 1	Chalcopyrite	-9.04	Marble (Bouhamra, Edough)
04 SK-CG	Pyrite	-7.44	Reaction skarn (Cap de Garde Edough)
01 MCG1	Pyrite	-9.9	Marble (Cap de Garde, Edough)
01MCG2	Pyrite	-17.4	Marble (Cap de Garde, Edough)
BMZ29-64	Pyrite	-8.1	Marble (Boumaiza, Edough)

The oxygen isotopic composition of garnets and clinopyroxenes from prograde skarn of Cycle II shows a narrow range of values between +8.4 and +9.9‰. The $\delta^{18}O$ of the two quartz minerals from the retrograde skarn yields similar values (+9.6‰ and +9.9‰). On the other hand, the skarn whole-rock sample exhibits a relatively lower $\delta^{18}O$ value (+6.5‰; Table 3).

$\delta^{13}C$ and $\delta^{18}O$ of the gangue calcite from retrograde skarn provide values of -6.0‰ and +15.9‰, respectively. However, those of the calcite from the host marble show clearly higher values of -4.2‰ and +25.7‰, respectively (Table 4).

Table 3- Oxygen isotopic composition of silicates from the Beleleita scheelite skarn.

Sample N°	Mineral	$\delta^{18}O_{V\text{-}SMOW}$ (‰)	Comments
ST2	Clinopyroxene	+9.9	Beleleita skarn
ST2	Clinopyroxene	+9.7	
TR1	Clinopyroxene	+9.3	
ST12	Clinopyroxene	+8.6	
ST13	Clinopyroxene	+9.4	
04 SK Ib	Clinopyroxene	+8.5	
TR1	Garnet	+9.2	
ST12	Garnet	+8.4	
ST13	Garnet	+9.5	
ST14	Quartz	+9.9	
TR1	Quartz	+9.6	
04 SK IIa	Whole-rock	+6.5	
Quartzite	Edough basement	+12.4	Edough basement

Table 4- Carbon and oxygen isotopic composition of carbonates from the Beleleita scheelite skarn.

Sample N°	$\delta^{13}C_{V\text{-}PDB}$ (‰)	$\delta^{18}O_{V\text{-}SMOW}$ (‰)	
TR1	-6.9	+15.9	Skarn calcite
BL-ca	-4.2	+25.7	Marble (Beleleita)

5. Interpretation and Discussion

5.1. Fluid Inclusions

In their fluid inclusion studies, Aissa et al. (1995, 1999, 2001) and Marignac et al. (2016) pointed out that the ore-forming fluids at Beleleita involved at least four hydrothermal end-members that underwent complex mixing-boiling processes, including the three FI types. The coexistence of diverse multiple immiscible phases of FIs is a typical pattern for the boiling process, as indicated to by Audétat (2019).

The (L+V)1 end-member is represented by FIs of high salinity (20 wt% NaCl–25 wt% NaCl) and high K/Na (~1.7) and Ca/Na (0.2 to 0.7) ratios. The (L+V)2 concerns FIs of relatively low salinity (< 15 wt% NaCl). The (L+V)1 and (L+V)2 end-members were mixed with carbonic-rich-fluid and CH_4- and N_2-bearing fluid, respectively, to produce the remaining two end-members.

Using H_2O-NaCl system of Bodnar et al. (1985), within the range of T_h from 350°C to 550°C, the corresponding pressures vary between 200–700 bars. Aissa (1997) and Marignac et al. (2016) used a combination of approaches to decipher thermobarometric (P-T) conditions, such as the transformation of lollingite to arsenopyrite and fluid inclusion data. For example, for the retrograde stage of Cycle II, the constructed isochores for the liquid-dominated (Type I) and vapor-dominant (Type II) FIs (Figure 8) trapping temperatures are 370°C–420°C and 420°C–450 °C, respectively. The estimated pressure range is between 350–650 bars. These results are consistent with those obtained from the reaction pair of lollingite and arsenopyrite. The estimated homogenised temperatures are particularly identical to most W-skarn deposits (between 400°C–600°C; e.g., Singoyi and Zaw, 2001; Orhan, 2017; Figures 7 and 8).

The moderate to high salinities as well as high K/Na (~1.7) and Ca/Na ratios point to a magmatic origin (e.g., Horn and Wickman, 1973; Singoyi and Zaw, 2001; Meinert et al., 2003; Orhan, 2017; Caldevilla et al., 2023). It is likely that the W, Li, F, and As inputs that characterise the Cycle II skarns were also caused by this magmatic fluid, which is well supported by the deposition of lithium- and fluorine-bearing minerals during the prograde stage of Cycle II.

The first melting temperatures are often very low and indicate a complex system with Na- and K-chlorides and divalent cations (Ca, Fe) equilibrated with highly saline fluid that is most likely a magma-derived source. According to Roedder (1984), the T_e of salt-dominated FIs are NaCl, T_e = -21.2°C, $CaCl_2$, T_e = -33.6°C and MgCl, T_e = -33.6 °C.

The wide range of salinity values and homogenisation temperatures recorded in the Beleleita W-As skarn is also observed in magmatic-hydrothermal systems for many skarn-related mineralisations (e.g., Baker and Lang, 2003; Li et al., 2019) and could be the result of a complex genetic mineralising process. Mixing low-salinity fluids causes a decline in salinities to mid-range values (which is the case in this study

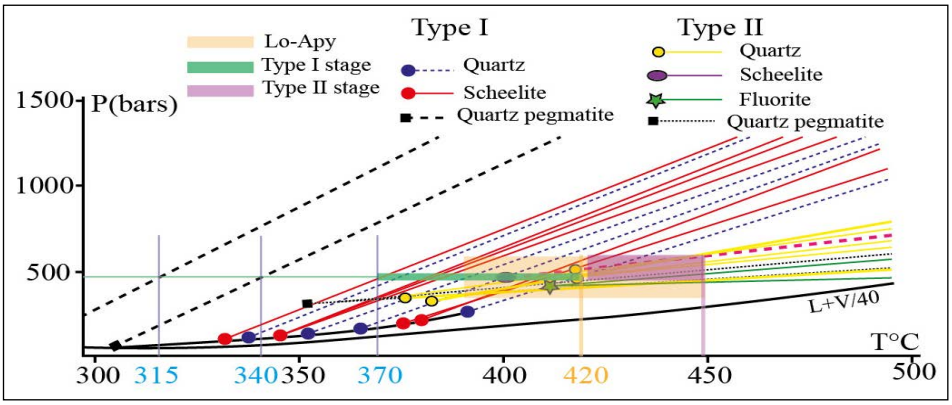

Figure 8- Thermo-barometric (P-T) estimation of the Beleleita skarn formation (Marignac et al., 2016). Lo = Lollingite; Apy = Arsenopyrite.

for low salinity FIs). Boiling is supported by scheelite precipitation at the end of the skarn episode as well as the coexistence of volatile-rich FIs and solid-rich FIs. Many similar studies (e.g., Li et al., 2016, 2019; Zhang et al., 2022*a*, *b*) have outlined boiling and causative phase separation as a significant mechanism of scheelite precipitation during metasomatism.

The volatile-rich fluids, which are characterised by high CH_4, N_2, and CO_2 contents, are likely to be of country rock (metamorphic) derivation. The occurrence of bismuth among the ore minerals may support the contribution of the country rock through chemical element leaching since the source of bismuth is often of sedimentary origin (Jiang et al., 2018). The abundance of CO_2, as well as CH_4 and N_2, is an indication of the redox state of the fluids that later deposited the W-Sn mineralisation (Gibert et al., 1992). This is well supported by the reduced character of the Beleleita skarn mineral assemblages, such as Pyrrhotite occurrence during both early and late skarn paragenesis, which indicates that skarnification and ore deposition were produced under reducing conditions from the beginning to the end of metasomatism. However, there is a lack of molybdenite in the ore assemblages.

5.2. Stable Isotopes

5.2.1. Sulphur Isotopes

The relatively narrow range of $\delta^{34}S$ values (from -0.3 to +1.8‰) in the main skarn sulphide mineralisation (pyrite and chalcopyrite of Cycle II; see Figure 9a) from Beleleita reflects a single sulphur source region. They are close to the MORB-type mantle values (-1.57‰ and +0.6‰) of Labidi et al. (2014) and are similar to many mantle-derived sulphurs (0 ± 3‰; e.g., Kyser et al., 1986; Ohmoto, 1986; Hoefs, 2009; Wei et al., 2019; Figure 8a). However, the MORB-type mantle values are dominated by negative values (mean $\delta^{34}S$ values = -0.64‰ ± 0.40‰; Labidi et al., 2014), while the $\delta^{34}S$ values of the Beleleita skarn sulphides are dominated by positive values (Table 1), with a single sulphur-rich lollingite sample that gave a $\delta^{34}S$ value of +5.2‰. The shift towards positive $\delta^{34}S$ values may reflect the incorporation of ^{34}S-enriched sulphur from an external source. Sulphide samples from the Edough marbles, whether at Beleleita or elsewhere in the metamorphic complex, gave large negative $\delta^{34}S$ values of -7.4 to -17.4‰, whatever the sulphide phases (pyrrhotite, chalcopyrite or pyrite; Laouar et al., 2002). These values most likely reflect the S-isotopic composition of the country metasedimentary sulphur. Thus, the positive $\delta^{34}S$ values of the Beleleita skarn sulphide sulphur cannot originate from the metamorphic country rocks; rather, the seawater sulphates of the Miocene period ($\delta^{34}S$ values between +21 and +23‰; e.g., Paytan et al., 1998; Present et al., 2020; Figure 9c) are the most likely contaminating source. This is supported by the fluid inclusion studies carried out by Aissa et al. (1995) on magmatic-related ore deposits of the Edough complex, where the hot (200°C to 500°C) magmatic nature of the mineralising fluids reflects the occurrence of seawater as a component of the studied fluid inclusions. Furthermore, the S-isotopic data observed in the Edough and Cap de Fer Miocene igneous rocks show $\delta^{34}S$ values varying between -3.6 and +9.1‰ (Figure 9c) and related mineralisation varying between -3.0 and +5.1‰; these were interpreted by Laouar et al. (2002, 2005) as mantle-dominated sulphur sources. Interaction of the igneous fluids with seawater would have shifted the mantle S-isotopic signature towards positive values (Laouar et al., 2002).

5.2.2. Oxygen Isotopes

$\delta^{18}O$ values of the garnet, clinopyroxene, and quartz minerals from the Beleleita skarns are in the range of +8.4 to +9.9‰ (Figure 9b). These values are clearly lower than those obtained from the quartzite sample of the Edough metamorphic complex ($\delta^{18}O$ value = +12.4‰) and lower than the oxygen isotopic composition of the metamorphic gneisses and micaschists of the massif ($\delta^{18}O$ ranging from +9.3 to +12.7‰) reported by Laouar et al. (2002; Figure 9d). However, they fall between the range of the Miocene I-type igneous rocks (diorites, microgranites, and rhyolites) $\delta^{18}O$ values of +6.2 to +6.9‰ (Laouar et al., 2002) as well as the range of the reaction skarns and micaschists (+10.3 to +12.7‰) of the Edough massif. Given that the obtained $\delta^{18}O$ values are close to those of the mantle peridotites and fresh basalts

from the mid-ocean ridges ($\delta^{18}O$ values range from 5 to 6‰), Laouar et al. (2002) interpreted the oxygen isotope data of the I-type granitoids of the Edough massif as reflecting a mantle-dominated signature similar to their S-isotopic compositions (e.g., Mattey et al., 1994; Xu et al., 2021). The interaction of the fluids originating from this magmatic event with the metamorphic marbles of the Beleleita would logically drive the oxygen isotopic composition of each reservoir towards the values of the other as the $\delta^{18}O$ value is exchanged, the extent of which depends on the temperature and water-rock ratio of the hydrothermal system (Taylor vd., 1997). Therefore, considering the observed $\delta^{18}O$ values, the skarnification process was most likely produced as the result of the interaction of fluid derived from the Miocene magmatic event with the marbles of the Beleleita. The oxygen isotopic composition of the skarn whole-rock sample yielded a value of +6.5‰. This low value could be attributed to the involvement of surface water during hydrothermal alteration since surface water — most likely the Miocene seawater indicated by fluid inclusion studies (see above) — exhibits generally negative values (mean $\delta^{18}O$ = -2.9 ± 0.4‰; Prasanna et al., 2021). At the same time, the similarity in the oxygen isotopic composition of garnet and pyroxene of prograde stage (Cycle I; from +8.4 to +9.9‰) and quartz of retrograde stage (Cycle II; +9.9‰) is an indication of the inheritance of the oxygen isotopic signature from a single source. This provides solid support for the fact that the fluid reacted continuously over a long period with the carbonate protolith to form the entire skarn. The low $\delta^{18}O$ values of the gangue calcite (+15‰) of the mineralised skarn relative to marble carbonates ($\delta^{18}O$ = +25.7‰) indicate different source regions of the oxygen, namely a hydrothermal origin for the former and a sedimentary signature for the latter.

5.2.3. Carbon Isotopes

The $\delta^{13}C$ of the marble calcite gave a value of -4.2‰, which is close to the values of marine inorganic carbon ($\delta^{13}C$ = -3 to +3‰; Bowman, 1998; Hoefs, 2009; Cai et al., 2023). However, a slight shift towards negative values could be attributed to mixing with a small amount of marine organic carbon during the diagenesis of these carbonate rocks. On the other hand, the gangue calcite is depleted in ^{13}C compared to the marble calcite, where $\delta^{13}C$ = -6.9‰. This depletion could be explained either by an input of organic ^{13}C-depleted carbon ($\delta^{13}C$ values of –20‰ to –30‰: e.g., Yeh and Epstein, 1981; Schoell, 1984; Berger and Vincent, 1986; Oehlert and Swart, 2014) into the mineralising fluids or by the calcite carbon originating directly from a deep igneous source (e.g., mantle-derived carbon ($\delta^{13}C$ values of –5 to –10‰: Ohmoto and Goldhaber, 1997). According to results of FI and stable S- and O-isotope studies, a large amount of the mineralising fluids in the Beleleita and Edough massifs originated from Tertiary magmatic hydrothermal events (Laouar et al., 2002). Thus, the carbon isotopic composition of the ore gangue calcite of the mineralised skarn might well be derived from a similar igneous source, giving the observed negative $\delta^{13}C$ value of -6.9‰.

6. Origin of the Metasomatizing and Ore-forming Fluid

Numerous geological studies have shown that the vast majority of the scheelite skarn form via the interaction between magmatic-derived fluids and carbonate rocks (e.g., Meinert, 1992; Chowdhury and Lentz, 2011; Huang et al., 2022). Their mineral phases, notably scheelite and garnet, inherit their metal contents from magmatic-derived fluids (Giuliani et al., 1987; Huang et al., 2022). The textural relationships of the Beleleita skarn indicate that the latest mineral assemblages were developed largely by pervasive and diffusive replacements of earlier assemblages and, to a lesser extent, by space-filling ores indicative of continuous pulses of metasomatism, similar to that observed in many skarns worldwide (e.g., Meinert, 1992; Kwak, 1994; Meinert et al., 2005; Wang et al., 2023). FI studies suggest mixing processes of magmatic-derived and metamorphic fluids for the precipitation of scheelite ore (Aissa et al., 1995, 1998, 1999; Marignac et al., 2016). In addition, the bi-cyclic development of the Beleleita scheelite skarn indicates a complex and long-lived metasomatic process. The mineral chemistries throughout the dominance of hedenbergite and grossular, in addition to pyrrhotite abundance, along with the deposition of (Mo-free) scheelite, are indicative of a reduced character of the

ore-forming fluid (Miranda et al., 2022). Moreover, the FI data indicate the involvement of volatile-rich and highly saline fluids (> 30 wt% NaCl) in mineralising Cycle II and belong to the H_2O-NaCl-KCl system equilibrated with magmatic-derived fluids. On the other hand, several low-salinity FI types and the presence of CH_4, N_2, and CO_2 reflect the contribution of metamorphic fluids. However, the high homogenization temperatures recorded (varying from 350 to 550°C) in skarn minerals (scheelite, fluorite, and quartz) point to a high-temperature ore-forming fluid source for both low- and high-salinity FI types. This supports the predominance of magmatic-derived sources with a minor metamorphic source contribution.

The observed homogeneity of the $\delta^{18}O$ signature of skarn paragenetic minerals (+8.4 to 9.9‰) falls within the igneous source of the skarnification fluid rather than the metamorphic origin since the $\delta^{18}O$ values of the latter are higher (> +12‰). In addition, Tornos et al. (2008) demonstrated that the $\delta^{18}O$ signature of skarn silicates is dominated by the inflowing fluid and that the proportion of oxygen retained from the protolith is negligible. The $\delta^{18}O$ data of the Beleleita skarn overlap with the interval of the $\delta^{18}O$ values from the neighbouring Miocene I-type granitoids in the Edough complex (Laouar et al., 2002) and are similar to the $\delta^{18}O$ values of the regional Los Santos scheelite skarn in Spain (Figure 9d).

The sulphur isotopic composition of the skarn sulphides yields values around 0‰, confirming the dominance of magmatic sulphur in the formation of the skarn ores. Again, the $\delta^{34}S$ data of the Beleleita skarn sulphides are similar to those of the sulphide mineralisation associated with the Edough igneous rocks (Laouar et al., 2002; Figure 9b).

Enrichment of late-stage paragenesis (Cycle II) with Li, As, Bi, and F, in addition to the observed high K/Na ratios, points to a hidden, largely differentiated igneous body whose fluids are responsible for skarnification and mineralisation processes (Aissa et al., 1995; Marignac et al., 2016). Marignac et al. (2020) highlighted similar conclusions when studying the world-class W-Sn deposit of Panasqueira (Central Portugal). The depth of this igneous body is estimated using FI (pressures of 0.5 kb to 0.6 kb) at 2 km to 2.5 km. The ore-forming fluids of the scheelite skarn deposit in the Beleleita area are largely dominated by a magmatic source, most likely derived from an I-type granite, and are petrographically and chemically similar to the granitoids of the Edough metamorphic complex. These fluids underwent complex mixing-boiling processes and were of high temperature, high salinity, and low oxygen fugacity.

7. Genetic Model of the Beleleita Scheelite Skarn

The Beleleita scheelite skarns are hosted by Neoproterozoic gneisses of the Edough metamorphic complex, which is a part of the internal zone of the North African Alpine belt. During the Upper Burdigalian, which marks a period of extensional orogenic events, the metamorphic complex and its cretaceous sedimentary cover were intruded by a number of igneous bodies that outcrop mainly at the northern part of the massif. These post-collisional calc-alkaline igneous rocks are thought to be mantle-derived, I-type granitoids (Laouar et al., 2002, 2005) emplaced within a subduction-collision regime. This environment was accompanied by hydrothermal fluids that migrate along faults and fracture zones towards the Earth's surface. These magmatic-derived fluids, which are characterised by high temperatures and high salinities, were responsible for cation leaching from the country rocks during their pathway upwards and may have been mixed with small amounts of crustal-derived fluids. The percolation of these hot and saline fluids at several pulses through the reactive marbles favoured the formation of calc-silicate rocks (skarns) and the deposition of W-As and sulphide mineralisation under reducing conditions. Figure 10 depicts the genetic model of the Beleleita scheelite skarns in relation to I-type igneous rocks of the Edough complex.

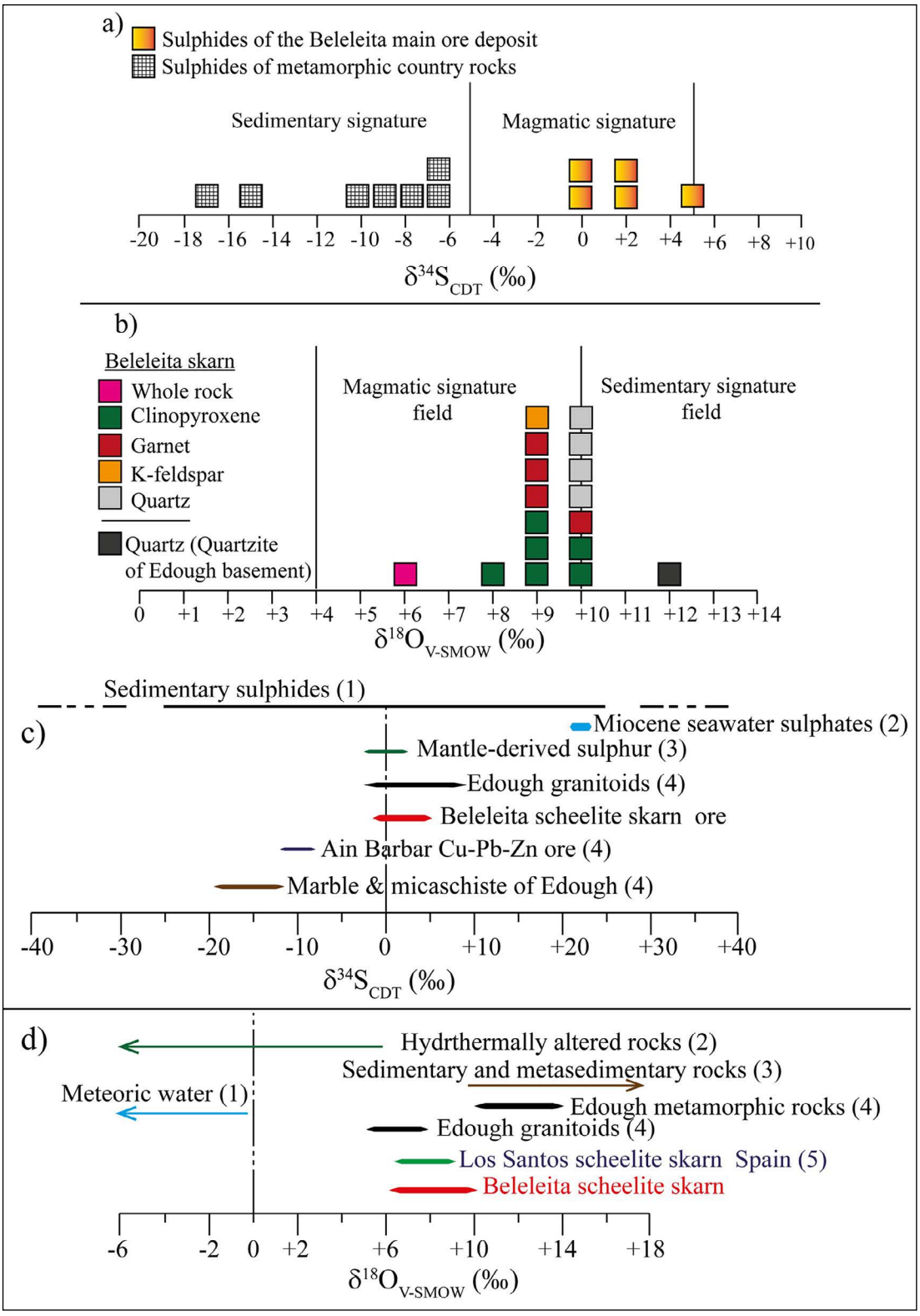

Figure 9- a) Histograms representation of sulphur isotope data from the scheelite skarn of Beleleita, b) Histograms representation of oxygen isotope data from the scheelite skarn of Beleleita, c) Comparison of sulphur isotopic composition of the Beleleita scheelite skarn with typical range of $\delta^{34}S$ of natural earth materials; (1) Coleman (1977) (2) Paytan et al. (1998) and Present et al. (2020), (3) Kyser et al. (1986) (4) Laouar et al. (2002, 2005), d) Comparison of the oxygen isotopic composition of the Beleleita scheelite skarn compared to those of typical earth materials and regional scheelite skarn examples, (1) Craig (1961), (2) Ohmoto (1986), (3) Taylor and Sheppard (1986) and Hoefs (2009), (4) Laouar et al. (2002), (5) Tornos et al. (2008).

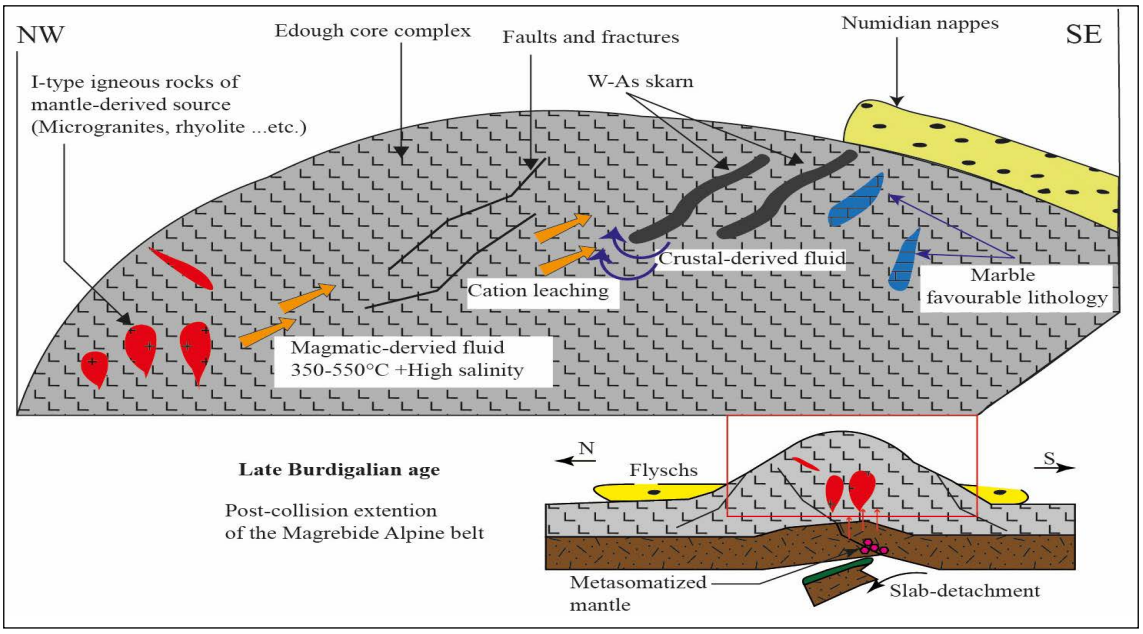

Figure 10- Genetic model for the Beleleita scheelite skarn showing the major role of the Late Burdigalian magmatic event in the formation of skarns and the deposition of the W-As related mineralisation.

8. Conclusion

The present study offers several conclusions:

- The Beleleita scheelite skarns formed during the Upper Burdigalian time are hosted by Neoproterozoic gneisses from the Edough metamorphic complex. These reduced percolation skarns and their related W-As-ore are believed to have formed as a result of two distinct metasomatic/hydrothermal cycles. Each cycle exhibits reduced mineralogical assemblages typical of numerous scheelite, Mo-free skarns worldwide. Hedenbergite, grossular, and plagioclase skarn minerals are in places wholly replaced by fluorine and lithium-bearing skarn parageneses (e.g., scheelite, fluorite, zinwaldite, Li-sphene), followed by silicate assemblages such as amphibole, epidote, quartz, and carbonates (calcite).

- Microthermometric measurements on FIs present high homogenisation temperature (T_h) values, ranging from 350 °C to 550 °C, and high salinities (> 30 wt% NaCl) typical for magmatic-derived fluids, with a minor contribution from the crustal component. W-mineralised skarns were formed at relatively low pressure (0.5 kb–0.6 kb).

- Stable S-, O-, and C-isotope investigations are consistent with FI data, reflecting large magmatic-derived ore-forming sulphur for sulphides, oxygen for silicates, and carbon and oxygen for gangue calcite. Minor crustal components are also indicated in the stable isotope data. Thus, we believe that the mineralising fluids in the Edough massif in the Beleleita region likely originated from a hidden I-type magmatic body located 2 km–2.5 km deep, as shown by FI data. The abundance of W and As, as well as the presence of volatiles such as Li and F, are indicative of the highly fractionated nature of the hidden igneous body.

Acknowledgement

Abdelmalek LEKOUI and co-authors are grateful for the anonymous reviewers, including editors, whose comments contributed to the improvement of the manuscript.

References

Abbassene, F., Chazot, G., Bellon, H., Bruguier, O., Ouabadi, A., Maury, R. C., Déverchère, J., Bosch, D., Monié, P. 2016. A 17 Ma onset for the postcollisional K-rich calc-alkaline magmatism in the Maghrebides, evidence from Bougaroun (northeastern Algeria) and geodynamic implications. Tectonophysics 674, 114–134.

Abbassene, F., Chazot, G., Bellon, H., Maury, R. C., Courme, M., Ouabadi, A., Coutelle, A. 2019.

New chronostratigraphic constraints on the emplacement of Miocene high-K calc-alkaline igneous rocks from West Edough-Cap de Fer, NE Algeria. Arabian Journal of Geosciences, 12 (2), 1-19.

Ahmed-Said, Y., Leake, B. E., Rogers, G. 1993. The petrology, geochemistry and petrogenesis of the Edough igneous rocks, Annaba, NE Algeria. Journal of African Earth Sciences (and the Middle East), 17(1), 111–123.

Aissa, D. E. 1996. Etude géologique, géochimique et métallogénique du massif de l'Edough (Annaba, NE Algérie). Thèse Doctorat Etat, 500. USTHB, Alger, Algeria (unpublished).

Aissa, D. E. 1997. Les minéralisations tertiaires de l'Edough (NE, Algérie) : métallogénie d'un 'metamorphic core complex' miocène. Doctorat thesis. Institute polytechnic of Lorraine 283, France. (unpublished).

Aissa, D. E., Cheilletz, A., Gasquet, D., Marignac, Ch. 1995. Alpine metamorphic core complexes and metallogenesis: The Edough case (NE Algeria). In: Pasava, J., Kribek, B., Zak, K. (Eds.), Mineral deposits: from their origin to their environmental impacts. Balkema, Rotterdam, 23–26.

Aissa, D. E, Marignac, Ch, Cheilletz A, Gasquet, D. 1998. Géologie et métallogénie sommaire du massif de l'Edough (NE Algérie). Mémoires Du Service Géologique d'Algérie, 9,7–55.

Aissa, D. E., Marignac Ch., Cheilletz, A., Gasquet, D. 1999. Le skarn à scheelite de Karezas (Annaba, Nord-Est Algérie): un skarn polycyclique d'âge burdigalien. Bulletin de Service Géologique d'Algérie, 10 (1), 3–53.

Aissa, D. E., Cheilletz, A., Marignac, Ch. 2001. Magmatic fluids and skarn mineralization: the Burdigalian W-As skarn at Karézas (Edough massif, NE Algeria). In: Piestrzyñski et al (Ed.) Mineral deposits at the beginning of the 21st Century. In: Proceedings of 6th Biennial SGA Meeting, Krakow, A.A. Balkema, Rotterdam, 877–880.

Audétat, A. 2019. The metal content of magmatic-hydrothermal fluids and its relationship to mineralization potential. Economic Geology, 114(6), 1033-1056.

Auzende, J. M., Bonnin, J., Olivet, J. L. 1975. La marge nordafricaine considérée comme marge active. Bulletin de la Société Géologique de France, 7(4), 486–495.

Baker, T., Lang, J. R. 2003. Reconciling fluid inclusion types, fluid processes, and fluid sources in skarns: an example from the Bismark Deposit, Mexico. Mineralium Deposita 38 (4), 474–495.

Berger, W. H., Vincent, E. 1986. Deep-sea carbonates: reading the carbon-isotope signal. Geologische Rundschau, 75 (1), 249-269.

Bodnar, R. J., Reynolds, T. J., Kuehn, C. A. 1985. Fluid-inclusion systematics in epithermal systems. Berger, B.R., and Bethker, P.m. (Eds.), Geology and Geochemistry of Epithermal Systems, Society of Economic Geologists. Littleton, USA, 73–97.

Bolfa, J. 1948. Contribution à l'étude des gites métallifères de la Kabylie de Collo et de la région de Bône. Bulletin du Service de la Carte Géologique de l'Algérie 6, 216.

Borthwick, J., Harmon, R. S. 1982. A note regarding CIF3 as an alternative to BrF5 for oxygen isotope analysis. Geochimica et Cosmochimica Acta, 46(9), 1665-1668.

Bosch, D., Hammor, D., Mechati, M., Fernandez, L., Bruguier, O., Caby, R., Verdoux, P. 2014. Geochemical study (major, trace elements and Pb–Sr–Nd isotopes) of mantle material obducted onto the North African margin (Edough Massif, North Eastern Algeria): Tethys fragments or lost remnants of the Liguro-Provençal basin? Tectonophysics, 626, 53–68.

Bouguerra, A. 1990. Etude des skarns et de la minéralisation associée dans le massif de l'Edough (cas du gisement As-W de Karésas comparée à l'indice de Bouzizi). These de Magister, Université de Constantine, 260, Constantine (Unpublished).

Bouillin, J. P. 1986. Le ''bassin maghrébin'': une ancienne limite entre l'Europe et l'Afrique à l'ouest des Alpes. Bulletin de la Société Géologique de France 8, II (4) 547–558.

Bowman, J. R. 1998. Stable-isotope systematics of skarn. In: Lentz, D.R. (Ed.), Mineralized Intrusion-Related Skarn Systems. Mineralogical Association of Canada. Short Course, Ottawa, 99-145.

Bruguier, O., Bosch, D., Caby, R., Vitale-Brovarone, A., Fernandez, L., Hammor, D., Laouar, R., Ouabadi, A., Abdallah, N., Mechati, M. 2017. Age of UHP metamorphism in the Western Mediterranean: insight from rutile and minute zircon inclusions in a diamond-bearing garnet megacryst (Edough Massif, NE Algeria). Earth and Planetary Science Letters, 474, 215-225.

Caby, R., Bruguier, O., Fernandez, L., Hammor, D., Bosch, D., Mechati, M., Laouar, R., Ouabadi, A., Abdallah, N., Douchet, C. 2014. Metamorphic diamonds in a garnet megacryst from the Edough Massif (Northeastern Algeria): recognition and geodynamic consequences. Tectonophysics, 637, 341-353.

Cai, Z., Yi, H., You, H. 2023. Carbon isotope stratigraphy across the Devonian–Carboniferous boundary

in the east Paleo-Tethys realm, Tibet, China. Minerals, 13(9): 1144.

Caldevilla, P., González-Menéndez, L., Martín-Crespo, T., Vindel, E., Guedes, A., Berrezueta, E., Gómez-Fernández, F. 2023. The Peña do Seo W-Sn deposit, NW Iberia: Petrology, fluid inclusions and OHS isotopes. Ore Geology Reviews, 155(19), 105361.

Carminati, E., Lustrino, M., Doglioni, C. 2012. Geodynamic evolution of the central and western Mediterranean: Tectonics vs. igneous petrology constraints: Tectonophysics, 579, 173-192.

Carminati, E., Wortel, M. J., Meijer, P. T., Sabadini, R. 1998. The two-stage opening of the western–central Mediterranean basins: a forward modeling test to a new evolutionary model. Earth and Planetary Science Letters, 160(3-4), 667–679.

Chowdhury S., Lentz, D. R. 2011. Mineralogical and geochemical characteristics of scheelite-bearing skarns, and genetic relations between skarn mineralization and petrogenesis of the associated granitoid pluton at Sargipali, Sundergarh District, Eastern India. Journal of Geochemical Exploration, 108 (1), 39-61.

Clayton, R. N., Mayeda, T. K. 1963. The use of bromine pentafluoride in the extraction of oxygen from oxides and silicates for isotopic analysis. Geochimica et cosmochimica acta, 27(1), 43-52.

Cohen, C. R. 1980. Plate tectonic model for the Oligo-Miocene evolution of the western Mediterranean. Tectonophysics, 68(3-4), 283– 311.

Coleman, M. L. 1977. Sulphur isotopes in petrology. Journal of the Geological Society of London, 133(6), 593–608.

Craig, H. 1961. Isotopic variations in meteoric waters. Science, 133 (3465), 1702–1703.

Durand-Delga, M. 1980. La méditerranée occidentale : Etapes de sa genèse et problèmes structuraux liés à celles-ci. Société Géologique de France, (10), 203- 224.

Einaudi, M. T., Burt, D. M. 1982. Introduction, terminology, classification, and composition of skarn deposits. Economic geology, 77(4), 745-754.

E.RE.M. 1969. Travaux de réévaluation du gisement à Sn-W de Beleleita. Rapport interne, (Inédit.).

Gibert, F., Moine, B., Schott, J., Dandurand, J. L. 1992. Modeling of the transport and deposition of tungsten in the scheelite-bearing calc-silicate gneisses of the Montagne Noire, France. Contributions to Mineralogy and Petrology, 112 (2-3), 371-384.

Giuliani, G., Cheilletz, A., Mechiche, M. 1987. Behaviour of REE during thermal metamorphism and hydrothermal infiltration associated with skarn and vein-type tungsten ore bodies in central Morocco. Chemical Geology. 64 (3-4), 279–294.

Hadj-Zobir, S., Oberhansli, R. 2013. The Sidi Mohamed peridotites (Edough massif, NE Algeria): evidence for an upper mantle origin. Journal of Earth System Science, 122 (6), 1455–1465.

Hammor, D. 1992. Du Panafricain au Miocene: 600 Ma d'évolution polycyclique dans le massif de l'Edough (Algerie nord-orientale) retracée par la pétrologie, la tectonique et la géochronologie (U/Pb, Rb/Sr, Sm/Nd,39Ar/40Ar). Nouvelle thèse, Université de Montpellier II, 205, France (unpublished).

Hoefs, J. 2009. Stable Isotope Geochemistry. Springer Verlag, Berlin, 286.

Horn, R. A., Wickman, F. E. 1973. The Na/K ratio of fluid inclusions in pegmatitic quartz and its genetic implications. A study by neutron activation analysis. Lithos, 6(4), 373-387.

Huang, X. D., Lu, J. J., Zhang, R. Q., Sizaret, S., Ma, D. S., Wang, R. C., Zhu, X., He, Z. Y. 2022. Garnet and scheelite chemistry of the Weijia tungsten deposit, South China: Implications for fluid evolution and W skarn mineralization in F-rich ore system. Ore Geology Reviews, 142, 1-18.

Ilavsky, J., Snopkova, P. 1987. Découverte d'Acritarches paléozoïques dans les terrains métamorphiques de l'Edough (Willaya d'Annaba, Algérie). Comptes rendus de l'Académie des sciences. Série 2, Mécanique, Physique, Chimie, Sciences de l'univers, Sciences de la Terre, 305(10), 881-884.

Jiang, W., Li, H., Evans, N. J., Wu, J., Cao, J. 2018. Metal Sources of World-Class Polymetallic W–Sn Skarns in the Nanling Range, South China: Granites versus Sedimentary Rocks. Minerals, 8(7), 265.

Kretschmar, U., Scott, S. D. 1976. Phase relations involving arsenopyrite in the system Fe-As-S and their application. Canadian mineralogist, 14 (3), 364-386.

Kwak, T. A. P. 1987. W-Sn skarn deposits and related metamorphic and granitoids. Elsevier, Amsterdam, 451.

Kwak, T. A. P. 1994. Hydrothermal alteration in carbonate-replacement deposits, Ore skarns and distal equivalents, in alteration and alteration processes associated with ore-forming systems. Lentz, D. R. (Ed.). Geological Association of Canada, short course notes, Ottawa, 381-402.

Kyser, T. K., Cameron, W. E., Nisbet, E. G. 1986. Boninite petrogenesis and alteration history: constraints

from stable isotope compositions of boninites from Cape Vogel, New Caledonia and Cyprus. Contributions to Mineralogy and Petrology, 93(2), 222-226.

Labidi, J., Cartigny, P., Hamelin, C., Moreira, M., Dosso, L. 2014. Sulfur isotope budget (^{32}S, ^{33}S, ^{34}S and ^{36}S) in Pacific-Antarctic ridge basalts: A record of mantle source heterogeneity and hydrothermal sulfide assimilation. Geochimica et Cosmochimica Acta, 133, 47-67.

Laouar, R. 2002. Petrogenetic and metallogenetic studies of the Tertiary igneous complexes of northeast Algeria: a stable isotope study. Doctorat d'Etat thesis, University Badji Mokhtar Annaba 171, Algeria.

Laouar, R., Boyce, A. J., Ahmed-Said, Y., Ouabadi, A., Fallick, A. E., Toubal, A. 2002. Stable isotope study of the igneous, metamorphic and mineralized rocks of the Edough complex, Annaba, Northeast Algeria. Journal of African Earth Sciences, 35(2), 271–283.

Laouar, R., Boyce, A. J., Arafa, M., Ouabadi, A., Fallick, A. E. 2005. Petrological, geochemical, and stable isotope constraints on the genesis of the Miocene igneous rocks of Chetaibi and Cap de Fer (NE Algeria). Journal of African Earth Sciences, 41(5), 445-465.

Li, J., Li, X., Xiao, R. 2019. Multiple-stage tungsten mineralization in the Silurian Jiepai W skarn deposit, South China: Insights from cathodoluminescence images, trace elements, and fluid inclusions of scheelite. Journal of Asian Earth Sciences, 181, 103898.

Li, X. F., Huang, C., Wang, C., Wang, L. 2016. Genesis of the Huangshaping W-Mo–Cu–Pb–Zn polymetallic deposit in Southeastern Hunan Province, Phina: constraints from fluid inclusions, trace elements, and isotopes. Ore Geology Reviews, 79, 1–25.

Marignac, Ch., Zimmermann, J. L. 1983. Âges K-Ar de l'évènement Hydrothermal et des Intrusions Associées dans le District Minéralisé Miocène d'Ain-Barbar (Est Constantinois, Algérie). Mineralium Deposita, 18 (3), 457–467.

Marignac, Ch., Aissa, D. E., Cheilletz, A., Gasquet, D. 2016. Edough-Cap de Fer Polymetallic District, Northeast Algeria: II. Metallogenic Evolution of a Late Miocene Metamorphic Core Complex in the Alpine Maghrebide Belt. M. Bouabdellah and J.F. Slack (eds.), Springer International Publishing Switzerland. Mineral Deposits of North Africa, 167-199.

Marignac, Ch., Cuney, M., Cathelineau, M., Lecomte, A., Carocci, E., Pinto, F. 2020. The Panasqueira rare metal granite suites and their involvement in the genesis of the world-class Panasqueira W–Sn–Cu vein deposit: a petrographic, mineralogical, and geochemical study. Minerals, 10(6), 1-47.

Mattey, D., Lowry, D., Macpherson, C. 1994. Oxygen isotope composition of mantle peridotite. Earth and Planetary Science Letters, 128 (3-4), 231–241.

Meinert, L. D. 1992. Skarns and Skarn Deposits. Geoscience Canada, 19 (4), 145-162.

Meinert, L. D., Hedenquist, J. W., Satoh, H., Matsuhisa, Y. 2003. Formation of anhydrous and hydrous skarn in Cu-Au ore deposits by magmatic fluids. Economic Geology, 98 (1), 147-156.

Meinert, L. D., Dipple, G. M., Nicolescu, S. 2005. World skarn deposits. In: Hedenquist, J. W., Thompson, J.F.H., Goldfarb, R.J., Richards, J.P. (Eds.), Economic Geology 100th Anniversary Volume. Society of Economic Geologists, Littleton, CO, 299–336.

Miranda, A. C. R., Beaudoin, G., Rottier, B. 2022. Scheelite chemistry from skarn systems: implications for ore-forming processes and mineral exploration. Mineralium Deposita, *57* (8), 1469-1497.

Newberry, R. J. 1998. W-and Sn-skarn deposits: a 1998 status report. Mineralized intrusion-related skarn systems, 289-335.

Oehlert, A., Swart, P. 2014. Interpreting carbonate and organic carbon isotope covariance in the sedimentary record. Nature Communications, 19 (5), 4672.

Ohmoto, H. 1986. Stable isotope geochemistry of ore deposits. Reviews in Mineralogy 16, 491–559.

Ohmoto, H., Goldhaber, M. B., 1997. Geochemistry of Hydrothermal Ore Deposits, third edition, 509–567.

Orhan, A. 2017. Evolution of the Mo-rich scheelite skarn mineralization at Kozbudaklar, Western Anatolia, Turkey: Evidence from mineral chemistry and fluid inclusions. Ore Geology Reviews, 80, 141–165.

Paytan, A., Kastner, M., Campbell, D., Thiemens, M. H. 1998. Sulfur isotopic composition of Cenozoic seawater sulfate. Science, 282, 1459-1462.

Prasanna, K., Ghosh, P., Eagle, R. A., Tripati, A., Kapur, V. V. Feeney, R. F., Fosu, B. R., Mishra, D. 2021. Temperature estimates of lower Miocene (Burdigalian) coastal water of Southern India using a revised otolith "clumped" isotope paleothermometer. Geochemistry, Geophysics, Geosystems, 22.

Present, T. M., Adkins, J. F., Fischer, W. W. 2020. Variability in sulfur isotope records of Phanerozoic seawater

sulfate. Geophysical Research Letters 47 (18), 1-17.

Roedder, E. 1984. The fluids in salt. American Mineralogist, 69 (5-6), 413-439.

Schoell, M. 1984. Recent advances in petroleum isotope geochemistry. Organic Geochemistry, 6, 645-663.

Singoyi, B., Zaw, K. 2001. A petrological and fluid inclusion study of magnetite–scheelite skarn mineralization at Kara, Northwestern Tasmania: implications for ore genesis. Chemical Geology. 173 (1-3), 239–253.

Soloviev, S. G., Kryazhev, S. G. 2018. Magmatic-hydrothermal evolution at the Lyangar redox-intermediate tungsten-molybdenum skarn deposit, western Uzbekistan, Tien Shan: Insights from igneous petrology, hydrothermal alteration, and fluid inclusion study, Lithos, 316, 154-177.

SO.NA.RE.M, 1975. Travaux d'exploration sur les minéralisations ferrifères du sud du massif de l'Edough. Rapport interne (unpublished).

Sterner, S. M., Hall, D. L., Bodnar, R. J. 1988. Synthetic fluid inclusions. V. Solubility relations in the system NaCl-KCl-H2O under vapor-saturated conditions. Geochimica et Cosmochimica Acta, 52 (5), 989-1005.

Taylor J. R., H. P., Sheppard, S. M. F. 1986. Igneous rocks: I. Processes of isotopic fractionation and isotopic systematics. Reviews in Mineralogy 16, 227–271.

Taylor, P., Larter, S., Jones, M., Dale, J., Horstad, I. 1997. The effect of oil-water-rock partitioning on the occurrence of alkylphenols in petroleum systems. Geochimica et cosmochimica acta, 61 (9), 1899-1910.

Tornos, F., Galindo, C., Crespo, J. L., Spiro, B. F. 2008. Geochemistry and origin of calcic tungsten-bearing skarns, Los Santos, Central Iberian zone, Spain. The Canadian Mineralogist, 46 (1), 87-109.

Wang, J., Zhao, L., Li, Q., Zhang, X., Wang, Y., Shao, Y., Li, Y. 2023. Ore-forming process of the W–Sn and Cu skarn mineralization in the Huangshaping deposit (Nanling Range): Constraints from scheelite geochemistry and cassiterite U–Pb geochronology. Ore Geology Reviews, 105354.

Wei, B., Wang C. Y., Lahaye Y., Xie L. H., Cao Y. H. 2019. S and C isotope constraints for mantle-derived sulfur source and organic carbon-induced sulfide saturation of magmatic Ni-Cu sulfide deposits in the Central Asian Orogenic Belt, North China. Economic Geology, 114 (4), 787-806.

Xu, J. Y., Giuliani, A., Li, Q. L., Lu, K., Melgarejo, J. C., Griffin, W. L. 2021. Light oxygen isotopes in mantle-derived magmas reflect assimilation of sub-continental lithospheric mantle material. Nature Communications, 12, 6295.

Xue, L., Wang, G., Tang, L., Cao, Y., Du, J., Du, Y., Cheng, H. 2021. Genesis and hydrothermal evolution of the Zhazigou skarn W (Mo) deposit, East Qinling, China: Constraints from fluid inclusions and H–O–S–Pb isotopes. Ore Geology Reviews, 138, 1-20.

Yeh, H. W., Epstein, S. 1981. Hydrogen and carbon isotopes of petroleum and related organic matter. Geochimica et Cosmochimica Acta, 45 (5), 753-762.

Zhang, Y., Chen, H. Y., Cheng, J. M., Tian, J., Zhang, L. J., Olin, P. 2022*a*. Pyrite geochemistry and its implications on Au-Cu skarn metallogeny: An example from the Jiguanzui deposit, Eastern China. American Mineralogy, 107 (10), 1910-1925.

Zhang, Y., Song, S. L., Hollings, P., Li, D. F., Shao, Y. J., Chen, H. Y., Zhao, L. J., Kamo, S., Jin, T. T., Yuan, L. L., Liu, Q. Q., Chen, S.C. 2022*b*. In-situ U-Pb geochronology of vesuvianite in skarn deposits. Chemical Geology, 612, 121-136.